NASA/TM-2002-211459

Aerothermal Instrumentation Loads To Implement Aeroassist Technology in Future Robotic and Human Missions to MARS and Other Locations Within the Solar System

Devendra S. Parmar
ICASE, Langley Research Center, Hampton, Virginia

Qamar A. Shams
Langley Research Center, Hampton, Virginia

April 2002

The NASA STI Program Office . . . in Profile

Since its founding, NASA has been dedicated to the advancement of aeronautics and space science. The NASA Scientific and Technical Information (STI) Program Office plays a key part in helping NASA maintain this important role.

The NASA STI Program Office is operated by Langley Research Center, the lead center for NASA's scientific and technical information. The NASA STI Program Office provides access to the NASA STI Database, the largest collection of aeronautical and space science STI in the world. The Program Office is also NASA's institutional mechanism for disseminating the results of its research and development activities. These results are published by NASA in the NASA STI Report Series, which includes the following report types:

- TECHNICAL PUBLICATION. Reports of completed research or a major significant phase of research that present the results of NASA programs and include extensive data or theoretical analysis. Includes compilations of significant scientific and technical data and information deemed to be of continuing reference value. NASA counterpart of peer-reviewed formal professional papers, but having less stringent limitations on manuscript length and extent of graphic presentations.

- TECHNICAL MEMORANDUM. Scientific and technical findings that are preliminary or of specialized interest, e.g., quick release reports, working papers, and bibliographies that contain minimal annotation. Does not contain extensive analysis.

- CONTRACTOR REPORT. Scientific and technical findings by NASA-sponsored contractors and grantees.

- CONFERENCE PUBLICATION. Collected papers from scientific and technical conferences, symposia, seminars, or other meetings sponsored or co-sponsored by NASA.

- SPECIAL PUBLICATION. Scientific, technical, or historical information from NASA programs, projects, and missions, often concerned with subjects having substantial public interest.

- TECHNICAL TRANSLATION. English-language translations of foreign scientific and technical material pertinent to NASA's mission.

Specialized services that complement the STI Program Office's diverse offerings include creating custom thesauri, building customized databases, organizing and publishing research results . . . even providing videos.

For more information about the NASA STI Program Office, see the following:

- Access the NASA STI Program Home Page at ***http://www.sti.nasa.gov***

- Email your question via the Internet to help@sti.nasa.gov

- Fax your question to the NASA STI Help Desk at (301) 621-0134

- Telephone the NASA STI Help Desk at (301) 621-0390

- Write to:
  NASA STI Help Desk
  NASA Center for AeroSpace Information
  7121 Standard Drive
  Hanover, MD 21076-1320

NASA/TM-2001-211459

Aerothermal Instrumentation Loads To Implement Aeroassist Technology in Future Robotic and Human Missions to MARS and Other Locations Within the Solar System

Devendra S. Parmar
ICASE, Langley Research Center, Hampton, Virginia

Qamar A. Shams
Langley Research Center, Hampton, Virginia

National Aeronautics and
Space Administration

Langley Research Center
Hampton, Virginia 23681-2199

April 2002

Acknowledgments

In writing this report, a tremendous amount of input from friends from industry and NASA has been forthcoming. Discussions with and suggestions from Mike Mitchell, Suen Kahng, Bob Blanchard, Bob Braun, and Peter Gnoffo of the Langley Research Center; Frank Milos of the Ames Research Center; David Spencer and Ram Ramesham of the Jet Propulsion Laboratory; Phillip Neudeck of the Glenn Research Center; R. H. Tolson of George Washington University; George Boctor of Kulite Semiconductor Products, Inc.; and Roger Blaser and Steve Tustain of Vibro-Meter SA have been very helpful.

Available from:

NASA Center for AeroSpace Information (CASI)
7121 Standard Drive
Hanover, MD 21076-1320
(301) 621-0390

National Technical Information Service (NTIS)
5285 Port Royal Road
Springfield, VA 22161-2171
(703) 605-6000

Abstract

The strategy of NASA to explore space objects in the vicinity of Earth and other planets of the solar system includes robotic and human missions. This strategy requires a road map for technology development that will support the robotic exploration and provide safety for the humans traveling to other celestial bodies. Aeroassist is one of the key elements of technology planning for the success of future robot and human exploration missions to Mars and to other celestial bodies. Measurement of aerothermodynamic parameters such as temperature, pressure, and acceleration is of prime importance for aeroassist technology implementation and for the safety and affordability of the mission. Instrumentation and methods to measure such parameters have been reviewed in this report in view of past practices, current commercial availability of instrumentation technology, and the prospects of improvement and upgrade according to the requirements. Analysis of the usability of each identified instrument in terms of cost for efficient weight-volume ratio, power requirement, accuracy, sample rates, and other appropriate metrics such as harsh environment survivability has been reported.

1. Introduction

For aeroassist technology, the identification of the state of the art and science of the instrumentation appropriate for aerothermal loads in hypersonic aeroassist environments is necessary. Plans or road maps for future NASA robotic and human flight missions are aimed at logical steps to create a required level of readiness for aeroassist technology to aid in the enhancement of planetary exploration for both advanced robotic and human missions. The most immediate strategic aim is exploration of Mars with six major robotic missions planned in the next 15 years. This new plan for exploring the nearest planet to Earth includes a mission to collect samples from the Martian surface and return them safely to Earth while maintaining the sample integrity. Accordingly the plan began with the launch of the 2001 Mars Odyssey on April 7, 2001. A pair of rovers that will move along the surface is proposed to be launched in 2003 with the launch of a scientific orbiter in 2005 and Mars samples obtained by 2011.

The logistics of a manned mission to another planet of the solar system are always complex; this is also true with the proposed robotic and crewed missions to Mars, the Red Planet. Many crucial issues must be considered before setting out into the solar system on the way to Mars. Some of these issues are transit vehicles and trajectories, crew safety and stay times, required resources and equipment, robotic functions, human-robotic interactions. Before any commitment to a human planetary exploration is made, studying and understanding these issues are essential to overcoming hazards that lie on the way to the destination. Basically the three elements of risk environment for human space missions are active space, in-space, and planetary surface environments. The active space environment, the highest risk segment of the mission, involves the energetics of the mission including the launch, orbital maneuvering, atmospheric entry to the host planet, and the atmospheric reentry to Earth. All these risk elements exist during the onward journey to the location, entry into its atmosphere, landing, and reentry into the atmosphere of Earth on return. The in-space environment segment of the mission comprises the time spent by the crew in transit to the location planet and subsequent return to Earth. This in-transit travel time poses the next greatest risk to crew safety because of radiation exposure and zero-gravity. Exposure to galactic cosmic rays and solar particle events are at a maximum while in transit and the detrimental effects of zero-gravity on the human body are fairly well-known. Exposure to the planetary surface environment involves the

time spent by the astronauts on the host planetary surface. On the Martian surface, the astronauts will experience gravity equal to about one third that on Earth ($0.38g$), and solar particle exposure will be considerably reduced because of the Martian atmosphere. This environment is also the one in which the understanding of the robot-astronaut interaction function is of primary importance.

The active space environment contains an inherent risk in any mission scenario, and extensive equipment-instrument testing is necessary to ensure crew safety during launch, maneuvering, and entry events. In this environment, the application of the key technology of aeroassist is used to enable or enhance planetary exploration. Implications of aeroassist technology application are known and include key aerothermal parameters. The purpose of this report is to identify such key aerothermal parameters and the technology for their measurement in terms of its state of the art and science, its application in past missions, and prospects for its future use. Temperature, pressure, and acceleration are the key aerothermal parameters identified and discussed in this report.

Numerous space exploratory missions have been made, and a tremendous amount of knowledge on some of our planetary neighbors is available. However, most of this knowledge is about the planetary atmosphere and its contents. Unfortunately, not much information is available about the hazards encountered on the way to the planets. Out of the many space exploratory missions, the Mars missions have been particularly useful in understanding the harshness of the environment experienced during orbital maneuvers. Out of more than 30 international attempts for Mars exploration, the Mars Global Surveyor and Pathfinder missions of NASA stand out in terms of obtaining useful aerothermodynamic data. The data acquired by the Mars Global Surveyor and Pathfinder missions have been extensively used in this report to understand the status of current technology of aerothermal data recording and its prospects for use in future robotic and human missions.

Thermocouples in conjunction with the platinum resistance thermometers have been consistently used to measure temperatures in NASA missions for planetary exploration as well as in the Apollo missions. The common practice has been to keep sensors and the recording electronics in a protected thermal box maintained at approximately a reference temperature inside the spacecraft. The hot junctions of thermocouples (standard K-type) are buried below the surface so that they are not exposed to the intense heat. The reference junction is kept in contact with the thermal box. Accelerometers and pressure sensors have never been installed near the surface because of their lack of survivability in a harsh environment. Surface pressures and temperatures are determined by extrapolation of the analyzed data recorded by sensors and instruments housed in the thermal box. The pressure on the spacecraft surface is usually determined by transmitting it to the sensor through insulated tubing connected to the pressure orifice mounted flush to the spacecraft surface. Such measurements introduce uncertainty in aerothermal data. For reliability and integrity of the aerothermal data, it is absolutely essential that the parameters be measured closest to the surface.

Technological information on current status of the aerothermal instrumentation for use in harsh environment has been presented and directions for further research and development in this area have been suggested. Aeroassist, a key technology, when implemented enables or enhances planetary exploration for both advanced robotic and human missions. This critical technique has been used in numerous space missions. It is therefore necessary to briefly discuss its critical elements and implications of its application.

2. Aeroassist Technology

Use of the atmosphere to achieve a critical function during aeroflight of a vehicle through atmosphere is referred to as "aeroassist" (ref. 1). Some of the critical elements of aeroassist technology are as follows:

Aerobraking

Aerocapture

Aeroentry

Aerogravity

Aeroassist has been used in past NASA missions, and the strategy is to implement it in future NASA missions. Some of the critical (present and future) missions include

Mars robotic missions—Mars Global Surveyor and Mars Sample Return Programs: 2001–2005

Mars Robotic Outpost Missions: 2007–2009

Solar System Exploration Missions—Neptune, Saturn, Titan: 2008–2009

Human Mars Missions: 2009 and beyond

Aeroassist is required for maneuverability during entry and descent for precision landing; human and instrument safety; safety, reliability, and integrity of the scientific data and samples; and cost-effectiveness and affordability of the mission. During the entry and landing phases of the aeroassist, the disciplines of aerodynamics and aerothermodynamics come into play, and the response is associated with temperature, dynamic pressure, and acceleration changes among many other factors.

2.1. Aerodynamic and Aerothermodynamic Implications

2.1.1. Aerobraking

Transition from an initial elliptical orbit to the circular science orbit is called aerobraking (refs. 1 to 14). Aerobraking uses atmospheric drag to effect orbit changes from initial elliptical to the desired circular science orbit. During the closest approach to the planet, atmospheric drag lowers spacecraft momentum. As the spacecraft slows during each drag pass, the orbit gradually lowers and becomes circular. Aerodynamic pressure, $(1/2)\rho V^2$ at periapsis (fig. 1), is one of the most important aerobraking parameters. Here ρ is the atmospheric density and V is the spacecraft velocity in the orbit. If $(1/2)\rho V^2$ is (1) too low, aerobraking takes too long or (2) too high, spacecraft damage is a possibility. This new capability of aerobraking has been used in space missions not to enter or leave orbit but to gradually modify the shape of the orbit by skimming through the high atmosphere.

2.1.1.1. Aerobraking phases. Aerobraking occurs in three primary phases:

Walk-in phase—during first 4–8 orbits following arrival

Main phase—begins at the point of the closest approach of the spacecraft to the planet, called orbit's periapsis (fig. 1)

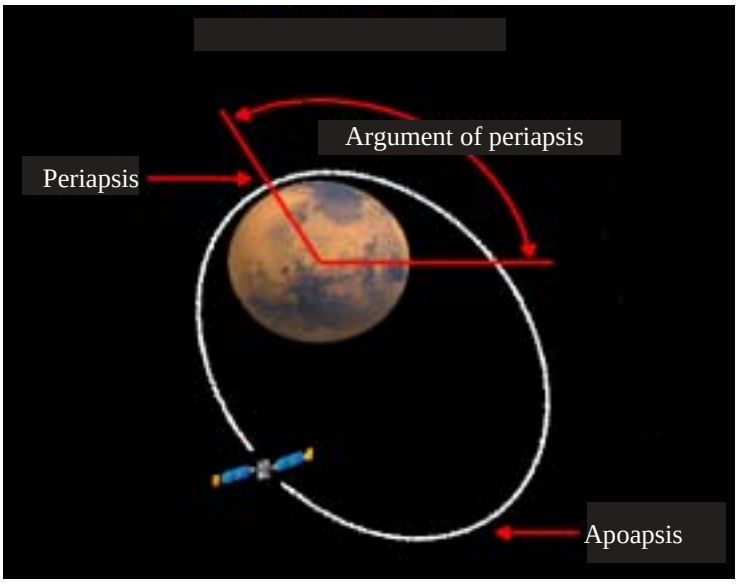

Figure 1. Orbital parameters 1 around Mars. (Photograph courtesy of Jet Propulsion Laboratory.)

Walk-out phase—occurs when the period of the spacecraft orbit is the shortest

Finally a transition from aerobraking to the beginning of the science orbit occurs.

2.1.1.2. Aerobraking missions. Aerobraking has been used in several space missions. Notables among them are (see fig. 2 for definitions of the parameters):

Magellan Mission to Venus 1993

Launched May 4, 1992; aerobraking was used in the spring of 1993. The parameters for aerobraking are shown in the following table:

Walk-in	Began on 5th orbit
Initial orbit	Eccentricity, e, 0.39
Inclination	85°
Periapsis	Altitude, 280 km; latitude, 10° N
Final orbit	e = 0.03; 70 days and 750 passes
Drag surfaces	Solar arrays
Limiting factor	Solar array heating

The dynamic pressure was estimated from the accelerometer data.

Mars 6 1973

USSR mission to Mars; not much information is available about it or the results, but we do know the following facts:

Had bus and descent module

Bus continued into heliocentric orbit after passing within 1600 km of Mars

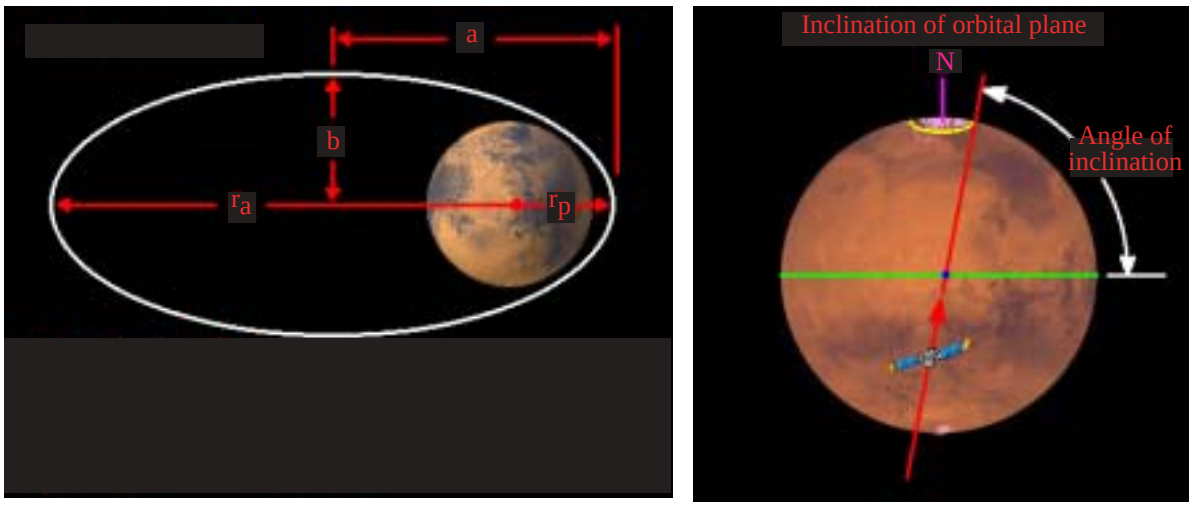

Figure 2. Orbital parameters 2 around Mars. (Photograph courtesy of Jet Propulsion Laboratory.) a = semimajor axis; b = semiminor axis; e = eccentricity = $(r_a - r_p)/(r_a + r_p)$; r_a = apogee radius = $a(1 + e)$; r_p = perigee radius = $a(1 - e)$.

Descent module entered the atmosphere at 5.6 km/s

Contact lost when the descent module, supposedly, hit the surface at 0.06 km/s

Mars Global Surveyor 1996

Launched November 7, 1996; entered Mars orbit September 1997 for aerobraking. The parameters for aerobraking are shown in the following table:

Walk-in	Began 5th orbit
Periapsis	Altitude, 128 km
Dynamic pressure:	
Actual	0.49 N/m^2
Desired	0.6 N/m^2
Atmospheric density:	
Actual	5 kg/km^3
Desired	60 kg/km^3
Knudsen number	0.2

At altitude of 110 km, dynamic pressure increased by 50 percent to 0.93 N/m^2 on orbit 15 because of solar panel deflection.

Dynamic pressure and density were estimated from accelerometer data.

2001 Mars Odyssey Mission

Launched April 7, 2001; arrived October 24, 2001; mass 758 kg (1671 lb), fueled; science instruments are Thermal Emission Imaging System (THEMIS); Gamma Ray Spectrometer (GRS); and Mars Radiation Environment Experiment (MARIE). (See fig. 3 for instrumentation.)

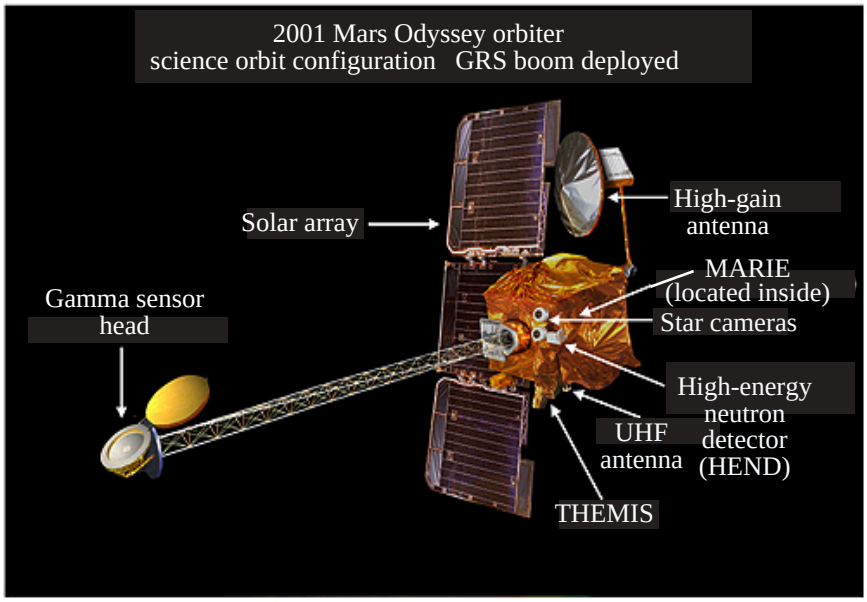

Figure 3. Schematic of 2001 Odyssey instrumentation. (Photograph courtesy of Jet Propulsion Laboratory.)

The proposed parameters for aerobraking implementation are as follows:

Periapsis of 100 km

Following aerobraking walk-out, orbiter will be in elliptical orbit with periapsis of 120 km and apoapsis near desired 400 km as for Mars Global Surveyor

Time for transition from aerobraking to science orbit is ≈1 week

Instrumentation similar to that on Mars Global Surveyor

Trajectory simulation requires 3 to 4 walk-outs (apoapsis, ≈450 km)

(For drag and trajectory configuration, see figs. 4 and 5.)

The proposal for the aerobraking for the Odyssey is that during each of its long, elliptical loops around Mars, the orbiter will pass through the upper layers of the Martian atmosphere each time it makes its closest approach to the planet. Frictional drag on the orbiter and its winglike solar arrays (figs. 4 and 5) because of planetary atmosphere will cause the aircraft to lose some of its orbital momentum during each close approach called "a drag pass." As the orbiter slows during each close approach, the orbit will gradually lower and become scientific (circular). Figure 5 shows the schematic of the Odyssey orbiter aerobraking and scientific payload details.

Future Mars Missions

Future Mars missions are anticipated to return samples of Mars dust and gas to Earth, employ a fleet of gliders to explore a Martian canyon, position small satellites to analyze the planet's atmosphere and weather, and rely on a surface rover to determine the age of rocks and soils.

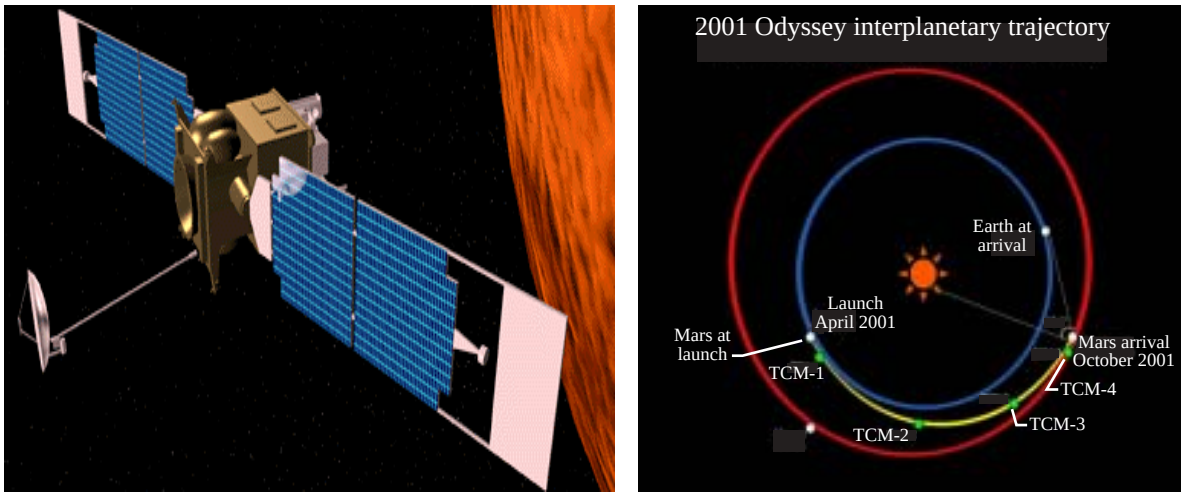

Figure 4. 2001 Odyssey solar panels and interplanetary trajectory around Mars. (Photograph courtesy of Jet Propulsion Laboratory.)

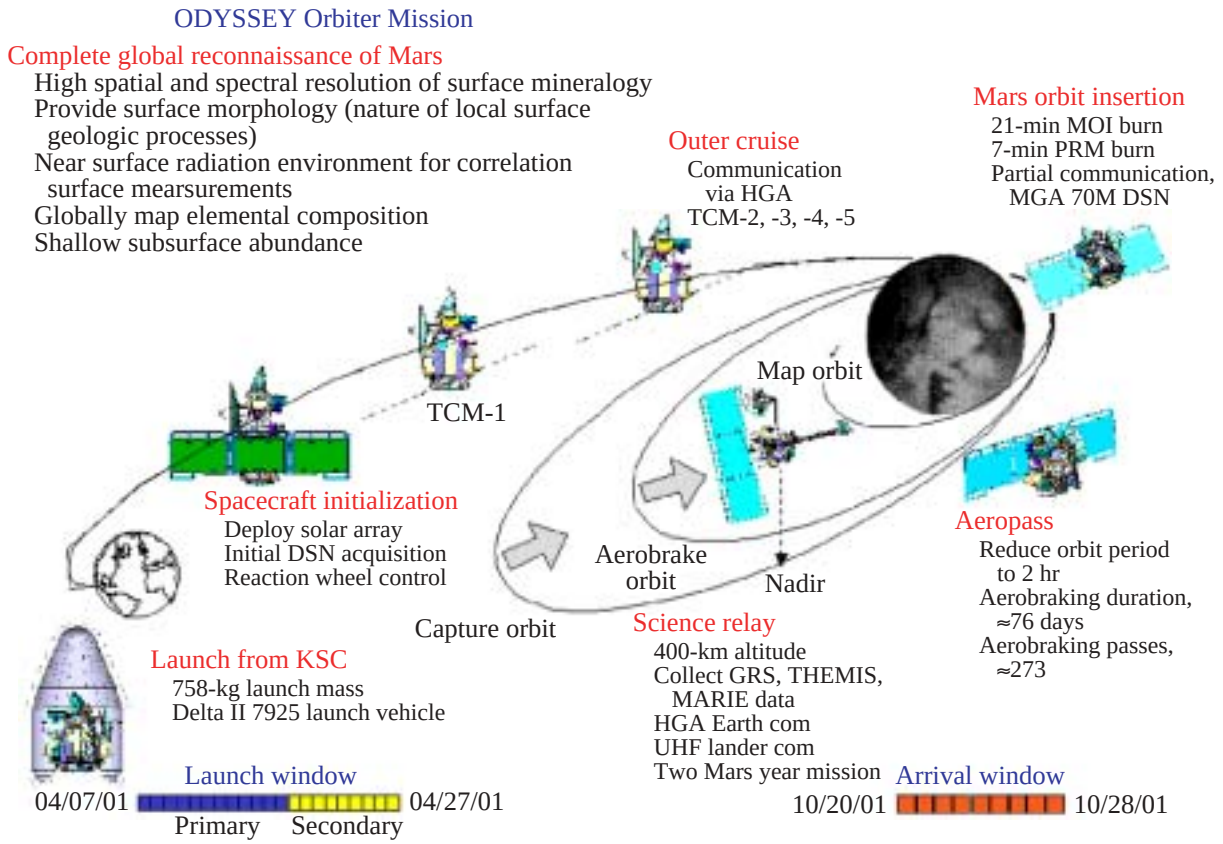

Figure 5. Schematic of 2001 Odyssey reconnaissance, science orbit, and instrumentation. (Photograph courtesy of Jet Propulsion Laboratory.)

2.1.2. Aerocapture

The uses and advantages of aerocapture are as follows:

Aerocapture is a technique to achieve precise captured orbit with single atmospheric pass

Can reduce or eliminate need for aerobraking

Can save significant amount of propellant

Enabling for most human missions

Planned to be used for first time on Mars Sample Return Orbiter, built by Centre National d'Etudes Spatiales (CNES), the French Space Agency, and is currently scheduled to be launched in 2005

For the proposed Sample Return Mission, which will use the Mars Sample Return Orbiter, an aerocapture maneuver will be used by arriving cargo and crew modules to enter an orbit around Mars. (See refs. 1 to 14.) In aerocapture, this maneuver is performed with the use of a single aeroshell which provides the aerodynamics and thermal protection needed for safe insertion into orbit. The main advantages of an aerocapture maneuver are the savings in spacecraft mass (an aeroshell is lighter than a propulsive capture stage) and the elimination of one propulsive stage (thereby potential risk on entry is minimized). Once the Mars orbit is captured successfully, a Mars descent maneuver will be performed. The aeroshell will provide thermal protection for the descending module during atmospheric entry. As the descending module enters the Martian atmosphere and slows considerably, the aeroshell will separate from the module and parachutes. Atmospheric propulsive maneuvers are likely to be used for vertical landing of the module on the surface. Extremely accurate surface delivery is required for all Mars surface payloads to ensure that all equipment intended for use during robotic and human missions is accessible upon arrival. An artist's concept of aerocapture technology is shown in figure 6.

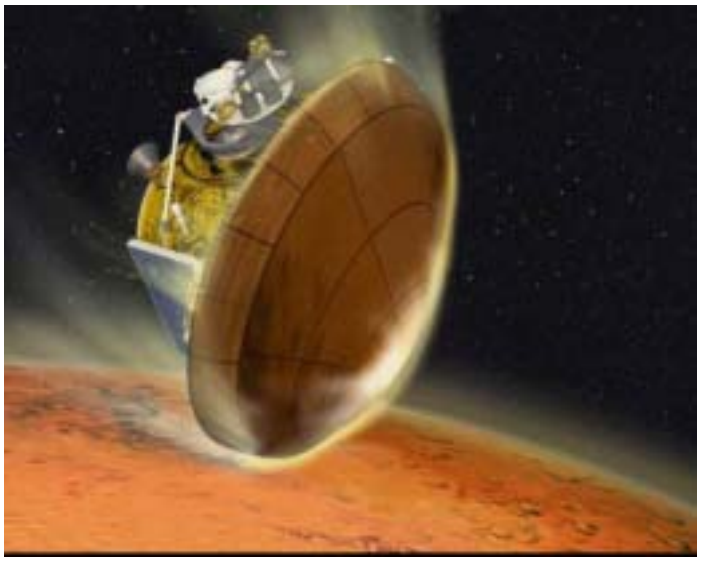

Figure 6. Artist's concept of aerocapture technology. (Photograph courtesy of Jet Propulsion Laboratory.)

2.1.3. Aeroentry

The technology of aeroentry is more common than either aerobraking or aerocapture. It is required whenever a vehicle descends to a surface that has an atmosphere. Viking, Mars Pathfinder, and Mars Polar Lander all performed aeroentries. Mars Surveyer '01 would have been the first lander on another planet to use a guidance algorithm to actively control the entry. Typical examples of aeroentry mechanisms are shown in figure 7.

2.1.4. Aerogravity Assist

For aerogravity assist, the vehicle uses a combination of atmosphere and propulsion to modify its hyperbolic orbit. Aerogravity assist is the use of aerodynamics and gravity for a larger bend angle; this technology allows smaller planets to be as effective as the larger planets for shortening the trip times. Low drag is required to minimize the loss in relative velocity during passage through the atmosphere; thus the contribution because of propulsion to velocity is minimal.

2.2. Aerodynamic and Aerothermodynamic Data From Mars Pathfinder Atmospheric Entry

2.2.1. Entry, Descent, and Landing

The following deceleration mechanisms were used for the Mars Pathfinder landing:

Aeroshell

Parachutes

Solid rockets

Airbags

The atmospheric velocity was 7.48 km/s; on the Mars surface it was 0 km/s. The peak heating rate was 100 W/cm^2, and peak deceleration was 16g (75–78 s after atmospheric entry).

Figure 7. An artist's concept of aeroentry technology. (Photograph courtesy of Jet Propulsion Laboratory.)

The entry, descent, and landing were made with an approach similar to that of the Viking Project in the 1970's, under the direction of LaRC and JPL.

2.2.2. Aeroshell

The aeroshell is the thermal protection system through the high-energy entry phase. Aeroshell housing to protect the sensors from the harsh environment was fabricated through a collaborative effort of JPL and Martin Marietta (now Lockheed Martin Corporation). The housing consisted of the three elements shown in table 1.

Table 1. Elements of Aeroshell Housing

Element	Manufacturer
Heatshield	Martin Marietta (now Lockheed Martin Corp.)
Backshell	JPL
Interface	JPL

2.2.3. Data From Atmospheric Entry Program (AEP) Instrumentation

Data were obtained from the following temperature sensors for the Atmospheric Entry Program (AEP):

9 type K thermocouples (TCs) with a temperature range of −270°C to 1270°C (calibration taken from ITS-90)

3 platinum resistance thermometers (PRTs)

TCs were mounted inside the aeroshell at various depths (0.4 to 1.34 cm) and PRTs were inside the structure. Sensors were not coplanar. TC1 was closest (0.4 cm) to the aeroshell surface; TC1, TC7, and TC8 did not give useful data. PRT2 gave inaccurate data. The measured dynamic pressure was 600 N/m^2, and the temperatures ranged from −58°C to 327°C ± 2.2°C.

2.2.4. Mars Pathfinder Atmospheric Entry

The predicted aeroshell surface peak temperatures for the Mars Pathfinder atmospheric entry are as follows (ref. 15):

100 percent laminar heating.....≈327°C after ≈100 s into atmospheric entry
85 percent laminar (scaled) heating.....≈227°C after ≈100 s into atmospheric entry
85 percent stagnation (scaled) point heating.....≈1727°C after ≈60 s into atmospheric entry

The heatshield material for the Mars Pathfinder was a graphite-epoxy composite (ref. 16) and the instruments included six thermocouples and three PRTs.

Six thermocouples were used with three for bondline measurements (stagnation, midcone, and edge of heatshield); two for middepth (stagnation and edge); and one for subsurface (stagnation). The thermocouples were installed in pairs to very tight tolerances (0.02 in. verified by x-ray) to allow temperature reconstruction as a function of depth. Only one thermocouple from a pair was connected for measurements. The thermocouple nearest the surface (stagnation point) failed. Peak heating at the stagnation

point was ≈90 W/cm^2 (determined from reconstruction of the entry trajectory by JPL and aerophysics codes from LaRC). The stagnation location measurements showed a temperature rise of 310°C (within 10°C of the predicted at the peak).

The actual entry and landing were accomplished on July 4, 1997. Entry interface conditions were as follows:

Radius	3522.2 km
Relative velocity	7.470 km/s
Relative flight path angle	−13.649°

Heatshield surface temperatures are predicted to change from 27°C to 1227°C (refs. 15 to 17).

2.2.5. Earth Entry Vehicles for Sample Return Missions

Vehicles which will be used for Sample Return Missions are Stardust, Genesis, Muses-C, Mars Sample Return Orbiter, and Comet Nucleus Sample Return. The entry velocities will be >11 km/s (for Stardust, 12.9 km/s; for Apollo Missions, 11 km/s). The heat flux will be approximately 1200 W/cm^2 at the stagnation point, and the peak surface temperatures at the stagnation point for an Earth entry vehicle is 3000°C (suggested heatshield material is phenolic impregnated carbob ablator (PICA), Ames Research Center).

3. Sensor Technology for Harsh Environment

Some examples of sensors for use in a harsh environment are depicted in figure 8. These include temperature sensors, SiC-based pressure and gas sensors, high-temperature accelerometers, and strain gauges.

3.1. Temperature Sensors

3.1.1. Thermocouples

Different types of standard thermocouples, their measurement range, and the materials are summarized in table 2. Although type B thermocouples cover the widest range of temperature, they do not cover enough below zero. Surface and atmospheric temperatures for most objects in our solar system are within the range of type K thermocouples; this is the primary reason for using type K thermocouples for temperature sensing in NASA missions. However, as the predicted temperatures during the entry, descent, and landing phases could cross the upper range covered by type K thermocouples and still be within the upper range of type B thermocouples, the recommendation is that both types, K and B, be installed and used simultaneously, instead of installing only type K in pairs and using only one of them at a time.

Table 2. Characteristics of Standard Thermocouples

TC type	Temperature range, °C	Material
B	0 to 1820	Pt-30 percent Rh versus Pt-6 percent Rh
E	−270 to 1000	Ni-Cr alloy versus Cu-Ni alloy
J	−210 to 1200	Fe versus another slightly different Cu-Ni alloy
K	−270 to 1372	Ni-Cr alloy versus Ni-Al alloy
N	−270 to 1300	Ni-Cr-Si alloy versus Ni-Si-Mg alloy
R	−50 to 1768	Pt-13 percent Rh versus Pt
S	−50 to 1768	Pt-10 percent Rh versus Pt
T	−270 to 400	Cu versus Cu-Ni alloy

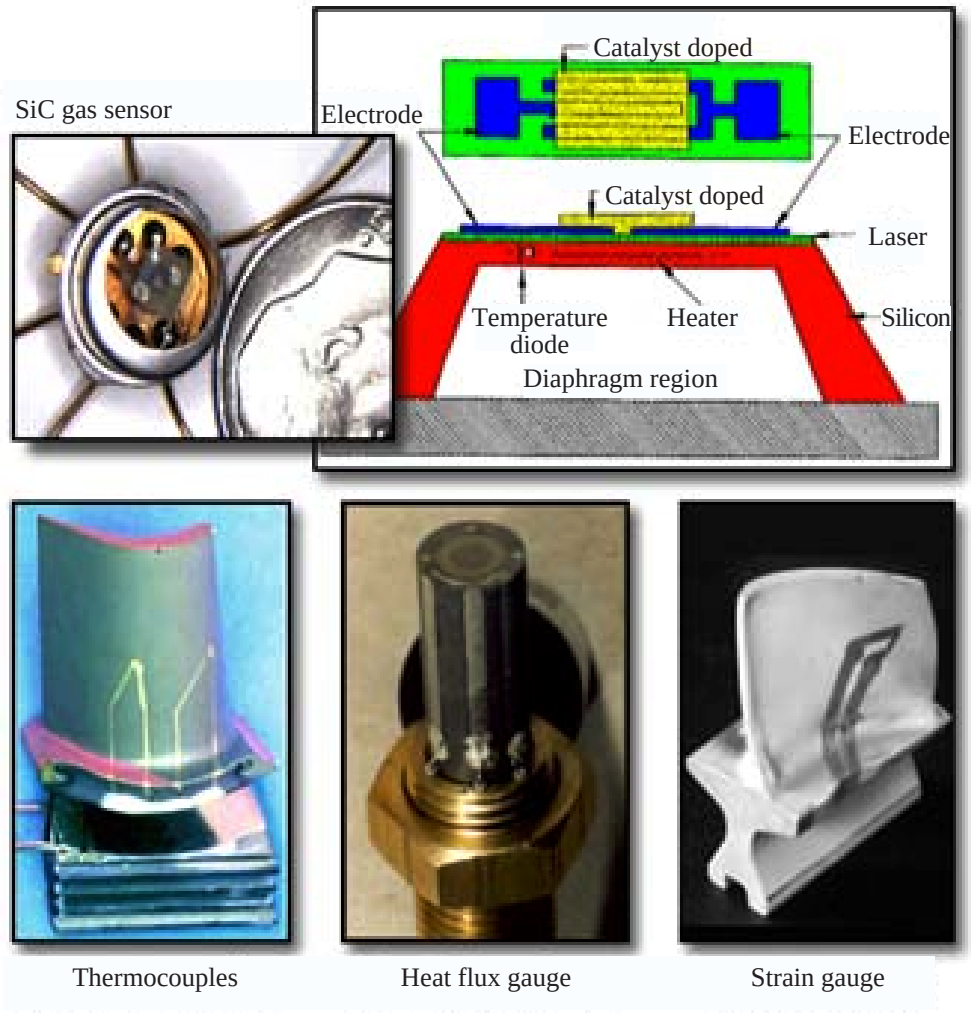

Figure 8. Examples of state of sensors for harsh environment.

Suppliers: Omega Engineering, Inc., Watlow Electric Manufacturing Company, and others

Federal stock numbers: 6145-00-LP0-1231; 6145-00-LP0-1232; 6145-00-LP0-1071

The sizes of type K and B thermocouples are given in table 3. Typical prices range from $17 to $36 (for five) for type K thermocouples and $16 to $191 (each) for type B thermocouples. Variation of thermal voltage with temperature for type K and B thermocouples is shown in figure 9. In the higher temperature range, the behavior of type B TCs is linear; this ensures better accuracy of aerothermal data during entry, descent, and landing.

Type B TCs are designed primarily to meet the temperature range of 1200ºC to 1800ºC; type B TCs should not be used in a reducing or reactive atmosphere. Type K (chromel-alumel) TCs are recommended by the ASTM for temperatures within the range from −250ºC to 1260ºC in oxidizing or inert atmosphere and up to 1350ºC for short periods. Reference junctions for data in figure 9 are at 0ºC.

Table 3. Thermocouple Size

TC type	Wire diameter, in.
K	0.0005
12 in. length	0.001
Standard	0.005
	0.010
	0.020
	0.032
B	0.008
6 in. length	0.010
Standard	0.015
	0.020
	0.032

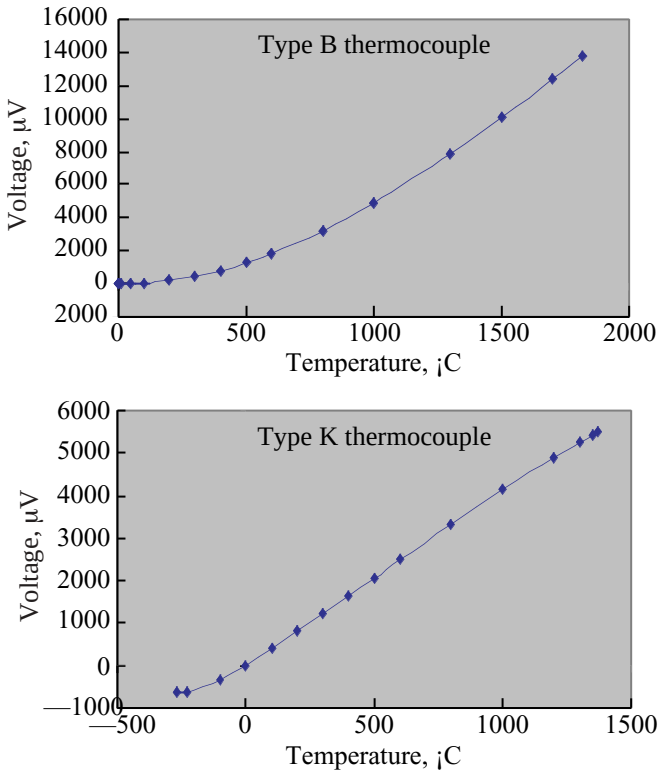

Figure 9. Temperature response of type K and B thermocouples.

3.1.2. Installation

In the past, TCs used thin wires custom-installed parallel to the surface to minimize temperature lag and heat conduction down the TC wires. The wires were welded, then the welded wiring was placed carefully onto a plug of the heatshield material. This assembly is then bonded into a hole in the heatshield so all that is seen are two wires coming from the inside surface of the heatshield. The wires pass through the structure if required and are connected to the data acquisition system. Heatshield materials were electrical insulators.

3.1.3. Data Acquisition

Thermocouple wires were routed to a nearby "isothermal block" (a chunk of aluminum) inside the structure that will change temperature slowly if at all. A PRT is attached with this block to measure the reference temperature needed to evaluate the thermovoltage with the help of an AST-MET 14-bit A/D converter and a derivative of the IBM 6000 computer that has a 32-bit architecture capable of executing 20 million instructions per second. The computer stores flight software as well as engineering and science data including images and rover information in 128 MB of RAM (random access memory). This processor and associated components are radiation hardened and mounted on a single electronic board. Data are transmitted to Earth and then converted to temperature.

3.2. Platinum Resistance Thermometers

The PRTs used were small platinum/ceramic devices ($4 \times 4 \times 1$ mm^3), Rosemount Aerospace Model 118MF (Rosemount Aerospace is now a subsidiary of Goodrich Corporation (formerly BF Goodrich)). Two PRTs were attached each to the fore and the aft aluminum blocks inside the structure. These aluminum blocks served as isothermal reference junctions for the TCs.

3.3. Accelerometers for Harsh Environment

3.3.1. Instruments in AST-MET Package

This AST-MET package consists of sensors on each of three spacecraft axes. The instrument is designed to measure accelerations over a wide variety ranging from microgravity experienced upon entering the atmosphere to the peak deceleration and landing events in the range of 30*g*–50*g*.

The accelerometer used was an Allied Signal Model QA3000 (Allied Signal has since merged with Honeywell International, Inc.).

The current accelerometers are Vibro-Meter piezoelectric accelerometers, type CA 250. (See appendix for more details.) The high-temperature capability is −269°C to +777°C; frequency response, 1 Hz–20 kHz; and sensitivity, 1 pC/g.

The weight of the accelerometer is 35 g and of the integral cable is 14 g/m. Different models are available that offer measuring ranges up to 5000*g* and 2900 psi. These accelerometers are qualified for flight on the Ariane 5 versatile launcher. They are delivered with a small charge converter (TCC 1XX) suited for the extreme high-temperature operation. These accelerometers are the extreme sensors in terms of survival capability (i.e., temperature, *g* level).

3.4. Pressure Sensors for Harsh Environment

Basically three types of high-temperature–high-pressure sensor technology are used:

Silicon diaphragm (piezoresistive) pressure sensors, which incorporate a fully active four-arm Wheatstone bridge dielectrically isolated silicon on silicon diaphragm

Silicon carbide (SiC) piezoresistive pressure sensors

High-temperature piezoelectric pressure sensors

3.4.1. Silicon Diaphragm (Piezoresistive) Pressure Sensors

Si-based sensors dominate the current industrial market because of the following unique Si characteristics:

1. Large piezoresistive coefficient, very high gauge factor, and compatibility with transistor fabrication techniques
2. Excellent transducer characteristics
3. High elastic modulus and low density
4. Low hysteresis because of single crystal nature of Si and superior thermal and environmental performance
5. Ability to be fabricated in small sizes with photolithography allows fabrication of very high resonant frequency devices
6. Integration of strain gauges and diaphragm in a single crystal eliminates bonding issues
7. Readily micromachinable using wet etch processes
8. Choice of crystallographic orientation and dopability
9. Applicability for on-chip integration of signal processing electronics (e.g., Si on insulator electronics operational to ≈250ºC)

Piezoresistive integrated sensor technology remains the leading transducer technology of the day. Requirements—particularly of the power generation, automobile, and space industries—for high-temperature pressure sensors based on piezoresistive pressure sensor principles determined the replacement of Si-based sensors with SiC-based sensors.

For semiconductor applications, silicon was originally adopted because of its large piezoresistive coefficient and compatibility with transistor fabrication techniques. However, in the middle 1950's, silicon was found to possess excellent transducer characteristics.

Si-based piezoresistive pressure transducers use the minute flexure characteristics of single-crystal silicon wafers, suitably doped for semiconduction, to effect a voltage proportional to pressure sensed on the face of the silicon wafer. The pressure sensitivity of the device is partly determined by micromachining the wafer to a thickness appropriate to the pressure range. The high elastic modulus and low density of silicon, along with the ability to be fabricated in very small sizes by photolithography, allow for a sensor with a very high resonant frequency, low hysteresis, and superior thermal and environmental performance.

The latest silicon technology of Kulite Semiconductor Products, Inc. consists of a monolithic structure composed of an atomically fused, dielectrically isolated, Wheatstone bridge integrated circuit fused onto a silicon substrate which acts as a force-summing diaphragm. This technology is known as dielectrically isolated "silicon-on-silicon" and exhibits excellent stability and thermal characteristics. However, transducers operate at temperatures up to 900ºF (482ºC) only and therefore are not suitable for hazardous conditions.

This technology was first used to manufacture tiny transducers used in wind tunnel, flight test, and acoustic measurements. These transducers quickly became an industry standard. Gradually this technology has replaced older bonded strain gauge and electromechanical designs in the aerospace and other industries where high reliability and rugged solid-state designs are desirable.

Kulite was the first to patent the silicon-on-silicon sensor (patent no. 4672354). This sensor is an evolution from the diffused semiconductor "first-generation" technology. It uses two silicon wafers bonded to but separated by a silicon oxide barrier. One wafer is chemically etched to make the Wheatstone bridge integrated circuit, the other is micromachined to provide the force collector, which translates the applied pressure into strain on the integrated circuit.

The benefits of using silicon-on-silicon pressure transducer technology are as follows:

1. Piezoresistive gauges are not mechanically glued or bonded to diaphragm or beam; devices are monolithic which significantly increases reliability and stability of sensor
2. High gauge factor, which means high sensor output, ranges from 100 to 300 mV typical
3. Single crystal silicon structure makes sensor inherently free of hysteresis
4. Single crystal silicon structure and packaging yield less than 0.1 percent drift per year of operation, which leads to long-term stability
5. Sensed media can be as high as 900°F (482°C); sensing element fabricated to provide small force collector; size and weight of finished transducer minimized
6. Dielectric isolation of sensing element means sensor will have dielectric strength above 500 V dc
7. Having no P-N junctions means sensor is not susceptible to electromagnetic interference (EMI) and has very low noise levels at elevated temperatures
8. Sensor is not electrostatic-discharge (ESD) sensitive

The following are some of the options the Kulite products offer:

High proof pressure capabilities: micromachined stops, 5 to 200 times overpressure, range dependent

Pressure ranges: 0–5 psi to 0–30000 psi (gauge, sealed gauge, absolute, differential)

High-temperature capabilities: +750°F (400°C) continuous operating, +650°F (343°C) compensated, no external cooling required

Low-temperature capabilities: cryogenic to −320°F (−196°C)

True gauge: transducers with ability to withstand hostile environmental conditions, medial isolation on the "measuring" port and reference side provided through the use of stainless diaphragms, particularly suited for changes in altitude

Bridge resistance: 1000 Ω (typical), or 350 Ω and higher resistances available upon request

High vibration capabilities: +100*g* rms with electronics

High unamplified output: standard, 100 mV; others, 150, 200, 300; low, 30, 50 mV

Amplified outputs available: 0–5 V dc, 1–5 V dc, 0–10 V dc, 1–9 V dc, 4–20 mA, others

Special amplified: transducer (0 to 5 V dc in/out potentiometer replacement)

Dual redundant sensor: 2 sensing elements in one transducer for redundant applications

LVDT replacement: solid state transducer offering LVDT V_1 and V_2 outputs

Shunt calibration

Submersible transducer/transmitters: for marine, water management, industrial, and applications

Flight qualified transducers: FAA authorized repair station

Many sizes: as small as 0.062-in. diameter by 0.20 in. long

Shape/configuration: to customer requirements

Pressure port: 6–32, 10–32, 3/8 in., 24 1/4 in. NPT, 7/16–20, virtually any thread size compatible with the unit size can be made, as well as specials such as flush face with O-ring seal

Electrical connections: cable output or connector

Pressure switches: custom designed for high vibration, hostile environments

Creep in Si at higher temperatures limits the use of Si pressure sensors to ≈450ºC. For a typical Si pressure, the creep time as a function of temperature is shown in figure 10. The creep time is significantly small beyond 450ºC.

3.4.2. Silicon Carbide Piezoresistive Pressure Sensors

SiC, because of the following unique characteristics, has the potential to overcome the Si limitations:

1. SiC is the only known binary compound of Si and C with excellent mechanical properties to very high temperatures
2. One-dimensional polymorphism and a relatively high gauge factor
3. Hard and chemically inert
4. Highly resistant to radiation damage
5. Wide energy band gap, ≈2.86 eV in 6H-SiC, high drift velocity, high electric breakdown strength, high thermal conductivity
6. Excellent material for high-temperature–high-pressure sensing and high-speed, high-power applications in hazardous environment

SiC characteristics and those of most commonly used semiconductors are shown in table 4 (6H-SiC, 4H-SiC, and 3H-SiC are different polytypes of SiC).

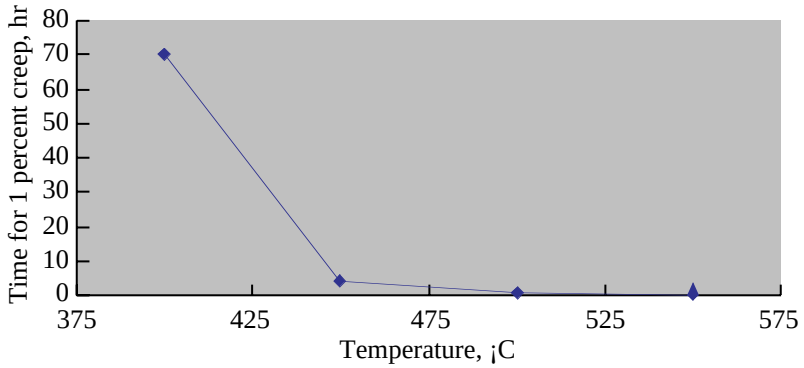

Figure 10. Variation of creep with temperature for typical Si pressure sensor.

Table 4. Characteristics of SiC and Most Commonly Used Semiconductors

Characteristic	Si	6H-SiC	4H-SiC	3H-SiC	Ga-As
E_g, eV	1.1	3.0	3.2	2.3	1.42
Breakdown electric field, 10^{17} cm^{-3} (MV/cm)	0.6	3.2	3	>1.5	0.6
Thermal conductivity, W/cm-K	1.5	4.9	4.9	5.0	0.5
Electron drift velocity, V, cm/s	10^7	2×10^7	2×10^7	2.5×10^7	10^7
Electron mobility, μ_e, 10^{16} (cm^2/V-s)	1100	370	800	750	6000
Hole mobility, μ_h, 10^{16} (cm^2/V-s)	420	90	115	40	320
Commercially available wafer size, in.	12	1.375	1.375	1.375	6

These SiC characteristics—namely, the exceptionally high breakdown field (>5 times that of Si), the wideband gap energy (>2 times that of Si), the high carrier saturation drift velocity (>2 times that of Si), and the high thermal conductivity (>3 times that of Si)—have potential to lead to substantial performance gains, in spite of its disadvantages due to low carrier mobility (ref. 18).

The superior intrinsic electrical properties of SiC have been known for decades, but fabrication of SiC wafers was not possible until recently. However, available SiC wafers lack reproducible properties of sufficient electrical quality for fabrication of advantageous devices and circuits. Efforts have been made to solve the problem of material shortage with the help of the process of heteroepitaxial growth of 3C-SiC on large-area substrates (primarily Si wafers). However, currently these efforts have not succeeded as the resulting SiC material still contains too many defects to be useful (ref. 19). Development of the modified Lely-seeded sublimation growth technique has the potential to provide acceptably large and reproducible single-crystal SiC wafers of usable electrical quality (refs. 20 to 22). One-in-diameter 6H-SiC wafers first became commercially available in 1989 (ref. 10). Since then a considerable SiC semiconductor device technology development has taken place and wafers up to 2 in. (50.8 mm ± 1 percent) in diameter and ≈254 μm ± 10 percent in thickness are now commercially available. 4H-SiC and 6H-SiC electronic devices presently exhibit the most promise because of availability and quality of reproducible single-crystal wafers in these polytypes. Further efforts are underway for development of 3-in. commercial SiC wafers. Westinghouse Science and Technology Center, Pittsburgh, PA, reported two important firsts in SiC wafer growth: the attainment of semi-insulating SiC wafers with resistivities in excess of 10^7 Ω-cm at room temperature and the realization of the first prototype 3-in. SiC wafers (ref. 23).

Table 4 clearly shows that 4H-SiC has substantially higher carrier mobility compared with 6H-SiC. Thus for electronic devices, this material should be the choice. However, for pressure sensing in a piezoresistive configuration, 6H-SiC would be suitable as well, although inherent mobility anisotropy that degrades conduction parallel to the crystallographic c-axis in 6H-SiC could be a cause of concern. If ongoing work ever solves the crystallographic defect problems associated with the heteroepitaxial growth of 3C-SiC on large-area Si substrates, foundry compatibility and economic advantages would conceivably push 3C-SiC to the forefront. HOYA Corporation, Tokyo, Japan, has developed 6-in. wafers of 3C-SiC.

At present, the chemical vapor deposition (CVD) growth technique shows the most promise for attaining epilayer reproducibility and throughputs for mass production of wafers (ref. 24). In-situ doping is primarily accomplished through the introduction of nitrogen (usually N_2) for n-type and aluminum (usually trimethyl- or triethylaluminum) for p-type gas species. A site-competition epitaxy technique that greatly enhances the range and control of in-situ doping of SiC during CVD growth was reported by Larkin et al. (refs. 25 and 26). Technological maturation via refined CVD reactor designs and growth

conditions is anticipated to address many problems in the near future. If downward trends in wafer prices continue, SiC technology development should accelerate and expand as SiC research efforts become more affordable.

Companies manufacturing or selling SiC wafers are as follows:

1. Sterling Semiconductors, 22660 Executive Drive, Suite 101, Sterling, VA 20166. Tel: (703) 834-7537 x205; Fax: (703) 834-7537; http://www.sterling.semiconductor.com; E-mail: sales@sterling.semiconductor.com
2. Cree Research, Inc., 4600 Silicon Drive, Durham, NC 27703. Tel: (919) 313-5300; Fax: (919) 313-5452; http://www.cree.com; E-mail: sales@cree.com
3. ATMI, Inc. (Advanced Technology Materials, Inc.), 7 Commerce Drive, Danbury, CT 06810. Tel: (203) 794-1100; Fax: (203) 792-8040; http://www.atmi.com; E-mail: info@atmi.com
4. SiCrystal AG, P.O. Box 3224, D-91020 Erlangen, Germany. Tel: +49 (0) 9131 / 73 33 97; Fax: +49 (0) 9131 / 73 22 37; http://www.sicrystal.de; E-mail: info@sicrystal.de
5. HOYA Corporation, 2-7-5 Naka-ochiai, Shinjuku-ku, Tokyo 161-8525 Japan Tel: (03) 3952-1151; Fax: (03) 3952-1314; http://www.hoya.co.jp; E-mail: info@mail.hoyausa.com

Specifications for 4H-SiC and 6H-SiC standard wafers are given in table 5 (ref. 27).

Table 5. Specifications for 4H-SiC and 6H-SiC Wafers

Property	Standard wafer	
	4H-SiC	6H-SiC
Diameter	34.9 ± 0.5 mm (1.4 in.)	50.8 ± 0.5 mm (2 in.)
Thickness	380 ± 50 μm	250 ± 25 μm
Dopant	Nitrogen	Nitrogen
Micropipe density	<50 cm^{-2}	<100 cm^{-2}
Usable area	>90 percent	>90 percent
Resistivity	≤0.020 Ω-cm	0.03–0.12 Ω-cm
Surface orientation	7.5° off axis; ±1° off towards	On-axis, ±0.5° 3.5° off axis ±1° towards
Surface	[a]Si or C face or both polished	[a]Si or C face or both polished
Edge exclusion	1 mm	1 mm
Orientation flat length	9.2 ± 2 mm	15.8 ± 1.5 mm
Identification flat length		8 ± 1 mm
Orientation flat orientation	Parallel {1 –1 0 0} ± 10°	Parallel {1 –1 0 0} ± 5°
Identification flat orientation		Si-face: 90° cw from orientation flat ±5° C-face: 90° ccw from orientation flat ±5°
Package	[b]FLUOROWARE®, single wafer packaged	[b]FLUOROWARE®, single wafer packaged

[a]Surface treatment as customer needs.
[b]Registered Trademark of Fluoroware, Inc. (now Entegris, Inc.).

For 4H-SiC standard wafers, the prices range from 485.00 EUR per wafer for 1–3 wafers to 370.00 EUR per wafer for more than 10. Also, there is an additional charge for both faces polished. For 6H-SiC

standard wafers, prices range from 1015.00 EUR for 1 wafer to 845.00 EUR per wafer for more than 10, with additional charge for polishing.

Single crystalline silicon carbide platelets are grown by the Lely method as material for required application. Lely material comes with low defect densities, high crystalline perfection, wide variety of polytypes, polished surfaces or KOH-etched surfaces, and as-grown surfaces (for 6H only). The specifications for Lely platelets are given in table 6.

Table 6. Specifications for Lely Platelets

Property	Lely platelets
Available polytypes	6H, 8H, 15R, 21R
Thickness	430–470 μm
Dopant	Nitrogen
Dopant concentration	N_D-N_A: $1.5 \times 10^{+18}$ cm^{-3} to $3.0 \times 10^{+18}$ cm^{-3}
Usable area, typical	6H: 50–100 mm^2 15R: 30–40 mm^2 21R: 30–40 mm^2
Surface orientation	On axis {0 0 0 1} ± 0.5°
Surface	Both sides polished Both sides polished, KOH-etched As-grown surface (6H only)
Package	Plastic container

Prices for Lely platelets range from 1.99 to 7.00 EUR per millimeter^2 of usable area, depending on polytype.

For more information on all these wafers, see references 27 to 29.

SiC is a potential candidate for use in wideband gap semiconductor, high-temperature radiation detection. SiC devices have demonstrated their operability as detectors for alpha particles, neutrons, gamma rays, and X rays at temperatures up to 700ºC and for prolonged times in intense neutron/gamma environments. They are being developed for many applications that include

Reactor excore power monitoring

Fuel assembly instrumentation

Fuel rod gamma scanning

Reactor core neutron monitoring during refueling operations

Transuranic waste tank dosimetry and monitoring

Recently, these detectors were applied successfully as part of a submersible fuel rod gamma scanner during measurements at an operating PWR fuel pool. This technology can also be used for high-temperature–high-pressure sensing. High-temperature application of SiC has been very well established in many other areas; some prominent high-temperature sensor applications of SiC are shown in the following table:

High-temperature application	Reason for application
Jet engine sensors, actuators, and control electronics	Sensor output signal amplification at high temperatures
Spacecraft power conditioning electronics and sensors	Reduce or eliminate need for cooling of engine electronics
Transmitters for deep well drilling	Aircraft weight savings; sensor amplification at point of measurement eliminates need for heavy shielding conduit for small signal transmission
Industrial process measurement and control instrumentation	Reliable sensing and control in aggressive environments not currently served by solid-state electronics
Distributorless electronic ignitions	Reduce size and weight of satellites and space platforms by allowing electronics to operate at higher temperature
Automotive engine sensors	Improved device reliability due to long-term chemical and thermal stability at elevated temperatures

Current technology status of SiC detectors is as follows:

1. Glenn Research Center and Semiconductor Products have demonstrated high-temperature–high-pressure sensitivity
2. GRC and Semiconductor Products high-temperature–high-pressure sensors could be modified for space applications
3. Kulite and GRC have demonstrated, both in bench and engine tests, SiC pressure sensitivity up to 500ºC in a nonhermetic package with a potential for use up to 650ºC and beyond in a hermetically sealed package
4. GRC has already demonstrated proper operation of prototype integrated SiC semiconductor electronic devices at temperatures as high as 650ºC
5. Deep reactive ion etching (RIE) has been demonstrated to be well-suited for micromachining of SiC for sensor development
6. Ohmic contacts at 500ºC have been demonstrated

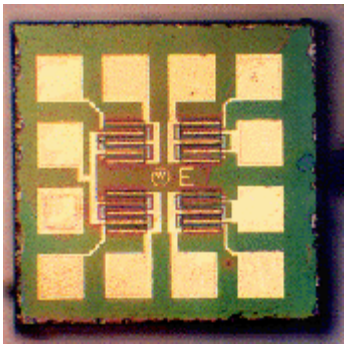

The primary technical challenges for SiC high-temperature–high-pressure use are as follows:

1. **Quality SiC single crystals**: Improvements in crystal growth and device fabrication processes are needed before SiC-based sensors can be scaled up and incorporated for space applications.

2. **High-temperature packaging**: Use of diamond films for thermal control of space electronics has been investigated at Glenn Research Center. Because diamond films have high conductivity, they can be used in spacecraft electronic packaging to increase density of microelectronics and reduce the mass and volume of power management and distribution system for a small spacecraft by up to 50 percent. Commercially available diamond films can be examined for use in packaging the SiC high-temperature–high-pressure sensors. Other high-temperature sensor packaging materials include metal/SiC composites.

Companies manufacturing diamond thin films and research efforts funded by U.S. government are as follows:

1. Diamonex, Incorporated (now Diamonex, Elm Division of Morgan Chemical Products, Inc.), 7331 William Avenue, Allentown, PA 18106. Tel: (610) 366-7100; Fax: (610) 366-7144
2. Advanced Technology Materials, Inc., 7 Commerce Drive, Danbury, CT 06810. Tel: (203) 794-1100; Fax: (203) 792-8040
3. CMC Wireless Corporation, 10409 South 50th Place, Phoenix, AZ 85044. Tel: (480) 496-5000; Fax: (480) 496-5060
4. Thermal Management Diamond Program through Defense Advanced Research Projects Agency (DARPA)

The performance and reliability of high-power defense electronics are limited by the inability of the associated microelectonics packages to dissipate heat. This limitation is becoming increasingly important as DOD moves toward more solid-state power devices. Because thin-film diamond substrates have more than five times the thermal conductivity of the alternative thermal management substrates, they can provide a significant advantage to many devices. The Thermal Management Diamond Program of DARPA is striving to overcome the critical barriers to the use of this material through lowering the processing cost of the diamond and demonstrating the use of diamonds in specific applications of interest to DOD.

The following Thermal Management Diamond Program efforts are being funded by DARPA:

$1/Carat CVD Diamond for Thermal Management (Applied Science and Technology, Inc.; Lockheed Sanders (now BAE Systems Information and Electronics Systems Integration Sector))

Defense Applications of Thermal Management Diamond (Hughes Space and Communications (now Boeing Satellite Systems))

Diamond Thermal Management Application for DOD Joint Tactical Information Distribution System (JTIDS) (Rockwell Collins)

Characterization, Diagnostics, and Modeling Support for Diamond (Naval Research Laboratory (NRL))

For more information on these efforts, see references 30 to 32.

Company manufacturing or selling metal/SiC composites is as follows:

dmc2 Electronic Components Corporation, P.O. Box 9409, 1300 Marrows Rd., Newark, DE 19714-9409. Tel: (302) 456-6300; Fax: (302) 456-6223

3. **High temperature ohmic contacts to SiC**: Relatively few attempts have been made to perform ohmic contacts to the 4H-SiC thin-film material. Most of these efforts have used Ni and Mo. Whereas the Ni contacts were annealed to 1000°C, higher temperatures in the 1000°C to 1600°C were utilized for Mo contacts. One of the most common and traditional methods of ohmic contact to both p- and n-type SiC has used alloying of SiC with tungsten at about 1900°C. For high-temperature–high-pressure sensor applications of SiC, thermal stability of the electrical contacts is of fundamental importance for reliable electronics and sensors operating in harsh environment. Aerospace propulsion systems typically encounter high-temperature, high-pressure, high-voltage, and extreme-vibration environments. Under such extreme conditions, the contact metallization undergoes irreversible microstructural changes that severely

degrade the device/sensor resulting in its failure. Aggressive packaging methodologies have been used to provide hermetic sealing against contact oxidation. These methods however add to the cost and the complexity of the system. It is imperative to test new methods and materials for the ohmic contacts to SiC sensors from the point of view of long-term contact stability and harsh environment survivability. These methods and materials need to be compatible and adaptable to the new strategy to couple interconnects, fabrication, micromachining, and packaging principles for achieving stable contacts on SiC sensors. The answer lies in the use of rare Earth metals for the purpose.

Glenn Research Center (GRC), with the support of Glennan Microsystems Initiative, has attempted to develop a thermochemical model of Ti/$TaSi_2$/Pt metallization on 6H-SiC and investigated the reaction kinetics of thermally stable contact after heat treatment in air up to 700°C. The metal contact surface morphology determined by using the scanning electron microscopy (SEM), high-resolution transmission electron microscopy (HRTEM), and the auger electron spectroscopy (AES) revealed a two-dimensional nonuniform oxide growth associated with the multigrain structure of the platinum overlayer (ref. 33). In these studies, the specific contact resistance values ranged from 10^{-6}–10^{-4} Ω-cm^2 and remained stable for 200 hr at 600°C in air. GRC proposes to use these results as a first step for future high-temperature SiC device implementation. Although platinum is required for the purpose of providing a protective silicide overlayer that is wettable for wire bonding apart from being conductive, its long-term stability needs to be established. These GRC investigations reveal thermally stability of the Ti/$TaSi^2$/Pt specific contact resistance after a long duration of exposure at 600°C in air.

4. **Micromachining of SiC**: The current technology for SiC device fabrication is based on the available technology for industrial Si microfabrication. However, SiC micromachining has unique advantages over Si micromachining in the sense that SiC thin film can be patterned easily by dry etching using Al masks. Further, SiC can withstand both KOH and HF etching. This feature is specially important considering the potential of SiC and diamond thin films and their process technology to fabricate microelectromechanical system (MEMS) devices necessary for high-temperature–high-pressure applications.

3.4.3. Piezoelectric Pressure Sensors

Ceramic piezoelements may be used up to 520ºC; for higher temperatures a natural crystal is necessary. The principal difficulty is achieving long-term reliability and stable characteristics for the sensor over the entire temperature range.

Methods to overcome this difficulty are as follows:

1. Locating the sensor in a cooler environment has been tested by many R&D teams worldwide including testing in generic missiles with Kulite pressure sensors. A drawback of this method is lower sensitivity to dynamic pressure due to the additional length of tube necessary to bring the pressure to the sensor. Also the response signal could be distorted due to possible acoustic resonance. Further, a response phase lag could occur and introduce a new, difficult parameter in the active control system and analysis.

2. Water-cooled devices are less reliable and more costly to implement. For vibrational level, an important concern in the choice of the pressure sensor, apart from the temperature range, is the acceleration sensitivity. Vibration compensating pressure sensors are now available. In piezoelectric pressure sensors, vibration compensation is done by using an internal acceleration-sensitive piezoelectric stack that is subtracted from the pressure and vibration sensitive stack. Lack of interchangeability of the piezoelectric pressure sensors is a drawback. These piezoelectric pressure

sensors cannot be calibrated or trimmed to a defined value. The pressure sensitivity is determined after assembly and depends on each crystal in the stack. For signal transmission, these pressure sensors require cables designed for piezoelectric devices. The cable needs to be a low-noise, low-capacitance, shielded, twisted-pair cable with high insulation impedance. For high-temperature applications, it should be able to withstand the change in temperature.

A low-noise differential charge amplifier optimized for high temperature is recommended for use with the sensor.

One piezoelectric pressure sensor for harsh environment is the Vibro-Meter CP 215, which has the following characteristics:

High-temperature capability ..... −196ºC to +780ºC
High-pressure capability ..... 350 bar
Frequency response ..... 2 Hz–15 kHz
Sensitivity ..... 25 pC/bar
Crystal element ..... VC2 type single crystal makes an extremely stable compression mode dynamic pressure transducer device
Linearity ..... ±1 percent over dynamic pressure range
Mounting ..... Flange
Weight
  Transducer ..... 12 g
  Integral cable ..... 25 g/m
Different models are available offering measuring ranges of 5000 *g* and 2900 psi
Qualified for flight on Ariane 5 versatile launcher
Delivered with small charge converter suited for extreme high-temperature operation
Extreme sensors in terms of survival capability (i.e., temperature, *g* level)
Compatibility with oxygen and hydrogen (in liquid and gaseous phases)

See appendix for more details.

4. Radiation Exposure Effects

In deep space, radiation exposure effects result largely from galactic cosmic rays and are anticipated to be significantly higher. Space radiation consists of electrons and ions (0.1–10 GeV/nucleon region) with ions passing through shield materials and fragmenting into nuclear constituents which generate new particles by nuclear collisions in the shield. The atomic collisions result in energy transfer to electrons associated with the colliding atoms (of the shield and the sensors near the surface).

Detailed studies have been made on the subject of radiation exposure shielding (e.g., ref. 34) and some of the recommendations are

Identification of newly developed materials (National Research Council and National Academy of Sciences reports)

High-performance material shields

In situ material utilization

Combination of materials for selective shielding

Dynamic shielding concepts

5. Other Proposed NASA Missions

Other proposed NASA missions are as follows:

Inside Jupiter

Proposed Launch: about 2006
Purpose: Study the internal structure of Jupiter

Inside Jupiter (short for interior structure and internal dynamical evolution of Jupiter) is a proposal under NASA Discovery Program of competitively selected missions. If selected in late 2001, it would be developed for launch about 5 years later. The spacecraft would orbit Jupiter to determine the internal structure of the giant planet by obtaining accurate, high-resolution maps of its magnetic and gravity fields. It would also examine processes occurring in the atmosphere and magnetosphere of Jupiter.

StarLight

Proposed Launch: July 2006
Purpose: To validate the technology of ultraprecision formation flying in space

StarLight will be the first time an "interferometer," a venture that combines the light from two optical telescopes to greatly multiply their observing power, will be launched into space. To achieve this goal, the telescopes must be carried on a pair of spacecraft flying in extremely precise formation. The mission will prove the technology required for the Terrestrial Planet Finder Mission, which will be designed to search for Earth-sized planets around other stars and look for the chemical signs of life. StarLight will use two small telescopes, each about the diameter of a bread plate. By combining their light using the technique of interferometry, StarLight will achieve the resolution of a telescope mirror 125 m (137 yd) in diameter—wider than the length of a football field.

Ball Aerospace and Technologies Corporation is the industrial partner for this JPL mission.

Space Interferometry Mission

Proposed Launch: 2009
Purpose: Space-based optical interferometer to study stars and detect extrasolar planets

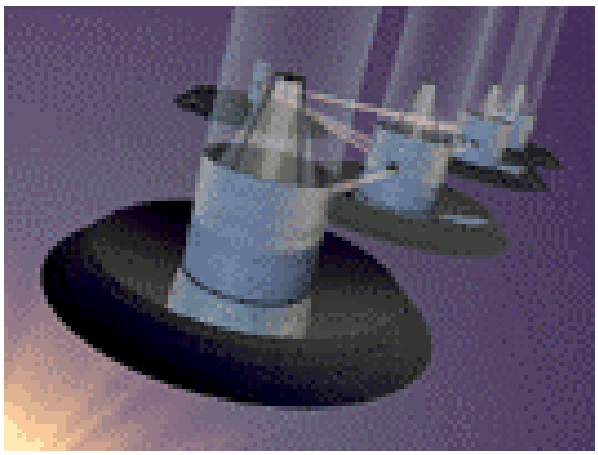

The Space Interferometry Mission (SIM) is an orbiting interferometer that will link multiple telescopes to function in unison as a much larger "virtual telescope." Its main goal is to detect planets of varying sizes—from huge planets the size of Jupiter to planets a few times as massive as Earth. It will do this by precisely locating nearby stars and looking for signs of any wobble, which may indicate that gravity from orbiting planets is tugging at them.

In addition, the mission will determine positions and distances to stars with an accuracy several hundred times greater than current telescope technology allows. This "street map" to our Milky Way galaxy could lead to breakthrough discoveries in astronomy. The mission will determine the distances to important signposts throughout the Milky Way, which will help us understand the universe, determine its age and size, and predict its future.

Partnering with JPL are TRW Inc. and Lockheed Martin Corporation, as well as numerous institutions represented on the science teams.

Terrestrial Planet Finder

Proposed Launch: 2012
Purpose: Space-based interferometer to search for Earthlike planets that might harbor life

Terrestrial Planet Finder will use multiple telescopes working together to take family portraits of stars and their orbiting planets and determine which planets may have the right chemistry to sustain life. The mission will study all aspects of planets, from their formation as disks of dust and gas around newly forming stars to their subsequent development. It will also look for planets orbiting the nearest stars and study their suitability as homes for any possible life. One great challenge is how to detect planets against the blinding glare of their parent star, an effort that has been compared with trying to find a firefly in the glare of a searchlight. By combining the high sensitivity of space telescopes with the sharply detailed pictures from an interferometer, Terrestrial Planet Finder will reduce the glare of parent stars by a factor of more than a hundred thousand to see planetary systems up to 50 light-years away.

Using spectroscopic instruments on Terrestrial Planet Finder, scientists will measure relative amounts of gases like carbon dioxide, water vapor, ozone, and methane. This study will help determine whether a planet may someday harbor life—or whether it already might.

Four companies have been selected to competitively develop mission concepts for the mission: Ball Aerospace and Technologies Corporation; Lockheed Martin Space Systems Company; TRW Inc.; and Boeing-SVS, Inc. About 75 scientists from 30 universities and research institutions, 16 industrial firms, and two NASA centers are represented on the teams.

6. Concluding Remarks

Thermocouples (B and K types) are the only available sensors for harsh environment temperature sensing. They need to be used simultaneously to cover a wider range of temperature change. High-temperature–high-pressure piezoelectric accelerometers are commercially available that cover a temperature range from −196°C to +777°C and acceleration up to 35*g*. High-temperature–high-pressure piezoelectric pressure transducers are commercially available to cover a temperature range from −196°C to +780°C and up to 350 bar. SiC technology for high-temperature–high-pressure piezoresistive pressure transducers is evolving and is still immature. However, it has great potential to revolutionize sensor technology for harsh environment. Packaging issues for harsh environment sensor electronics need to be resolved before SiC technology could be used. Research on diamond films for packaging is necessary. The spin-off of the SiC–diamond film processing technology would be in fabrication of microelectro-mechanical system (MEMS) devices for harsh environment applications. However, the question of the embedding of MEMS pressure and temperature sensors in the body of the heat shield still needs investigation.

Appendix

Specifications of Various Sensors

vibro-meter

DATA SHEET | Vibration 276-030

vibro-meter certified by

CA 250 M2XX
CA 250 M8XX

Piezoelectric Accelerometer Type CA 250 M2XX / M8XX

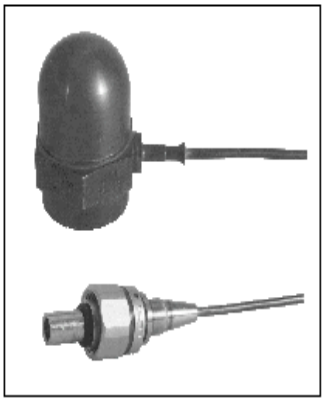

CHARACTERISTICS

- Qualified for flight on Ariane 5 versatile launcher (ESA-CNES-Snecma Moteurs-Arianespace Program)
- High-temperature capability -269°C to +777°C
- Differential stud eases integral cable mounting
- Proven reliability

FEATURES

- VC2 type crystal element
- Frequency response: 1 Hz to 20,000 Hz
- Sensitivity 1 pC/g

WEIGHT

Accelerometer : 35 g
Integral cable : 14 g/m

DESCRIPTION

The use of VC2 type single crystal material in the CA 250 compression mode accelerometer makes it an extremely stable device.

The transducer is designed for extremely high-temperature measurements. It is fitted with an integral mineral insulated cable (coaxial) which is terminated with a coaxial Lemo connector adapted by Vibro-Meter.

Where space is available for mounting the accelerometer with its integral cable, the standard MA 109 or MA 112 stud can be used. A unique MA 110 differential stud is available for mounting the CA 250 (M2XX / 8XX) accelerometer without having to rotate it.

CA 250 M2XX / M8XX

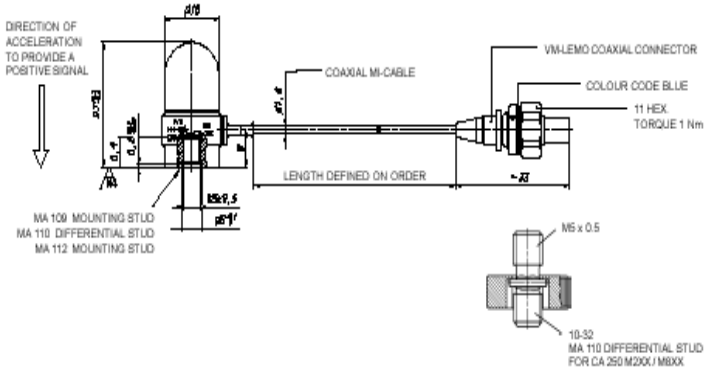

SPECIFICATIONS

CA 250 M2XX / M8XX

Input power requirements : None
Signal transmission : Unipolar system, charge output
Signal processing : Charge converter

OPERATING (at 23°C ±5°C)

Sensitivity (at 120 Hz) : 1 pC/g ±5%
Dynamic measuring range (random)
: 0.1 g to 5000 g peak
Overload capacity (spikes) : Up to 7000 g peak
Linearity : ±2% over dynamic measuring range, 1% up to 500 g
Transverse sensitivity : <5%
Resonant frequency (mounted)
: >48 kHz nominal

Frequency response
- 1 to 10,000 Hz nominal : ±5% (lower cutoff frequency is determined by the electronics and cable mounting)
- 20,000 Hz : <10%

Internal insulation resist. : Min. $10^8\Omega$

Capacitance
- Transducer : 120 pF nominal pole/ground
- Integral cable : 220 pF/m nominal pole/ground

ENVIRONMENTAL

Temperature range : -253°C to +727°C
Shock acceleration : <7000 g peak (half sine, 0.5ms) along sensitive axis
Pressure : <50 bar
Base strain sensitivity : <0.03 g/microstrain (with HP 0.3 Hz - 3 dB)
Acoustic sensitivity : (under 180 dB SPL) < 1 g RMS equivalent
Corrosion, humidity : Inconel 600, hermetically welded
Mounting : On surface roughness max. N4 (Ra≤0.2mm) stud 10-32 UNF2B or M5 x 0.5

CALIBRATION

Dynamic calibration at factory at 5 g peak and 120 Hz (+23°C). No subsequent calibration necessary.

Typical Responses

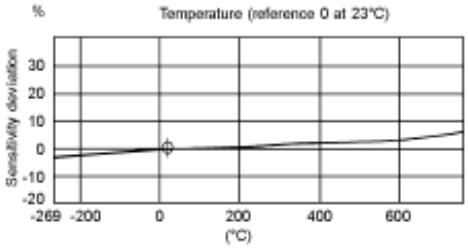

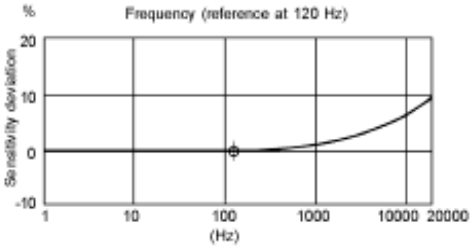

Accessories:

- Stud M5 x 0.5 / 10-32 MA 109 : See drawing 809-109-000 D 01
- Stud M5 x 0.5 / M5 x 0.5 MA 112 : See drawing 809-112-000 D 01
- Differential stud M5 x 0.5 / 10-32 MA 110 : See drawing 809-110-000 D 01
- Charge converter : See data sheet 278-002 TCC 1XX
- Softline cables EC 212 / 272 / 906 / 907 : See drawing 912-XXX-000 D011 as appropriate
- Triaxial mounting adaptor available

Ordering Information :

- Description / Ordering No : CA 250 / 144-250-000-2X Tapped hole M5 x 0.5
  - 1 cable length 1 m
  - 2 cable length 2 m
  - 3 cable length 3 m
  - 4 cable length 4 m
  - 5 cable length 5 m
  - 6 cable length 6 m

CA 250 / 144-250-000-8X Tapped hole M5 x 0.5
- 1 cable length 1 m
- 2 cable length 6 m

MA 109 / 809-109-000-01	Stud M5 / 10-32 for CA 250 M5 x 0.5
MA 110 / 809-110-000-01	Differential stud M5 / 10-32 for CA 250 M5 x 0.5
MA 112 / 809-112-000-01	Stud M5 / M5 x 0.5 for CA 250 M5 x 0.5
EC 212 / 272 / 906 / 907	See drawing 912-XXX-000 D011, as appropriate, for cable lengths and connector types

⚠ Due to the continual development of products, Vibro-Meter reserves the right to modify these specifications without forewarning.

vibro-meter

Head Office

Vibro-Meter SA, Rte de Moncor 4,
P.O. Box 1071, CH-1701 Fribourg, Switzerland
Phone : +41 26-407 11 11
Fax Industrial & Marine : +41 26-407 13 01
Fax Aerospace : +41 26-402 36 62
E-mail : vmsa@vibro-meter.ch
Internet : www.vibro-meter.com
www.meggitt.com

Sales Offices in :

- Germany
- France
- USA
- Canada
- Singapore
- United Kingdom
- Russia
- Ukraine

Agents in over 30 countries

Vibro-Meter is a member of the Meggitt Aerospace Systems Division

vibro meter

DATA SHEET | Dynamic Pressure 276-008

CP 215

vibro-meter certified by

Piezoelectric Pressure Transducer Type CP 215

CHARACTERISTICS

- Qualified for flight on Ariane 5 launcher (ESA-CNES-SEP-Arianespace Program)
- Extreme temperature capability -196°C to +780°C
- High-pressure capability 350 bar
- Compatible with gaseous and liquid oxygen and hydrogen
- Proven reliability

FEATURES

- VC2 type crystal element
- Frequency response: 2 Hz to 15,000 Hz
- Sensitivity 25 pC/bar

WEIGHT

Transducer : 12 g
Integral cable : 25 g/m

DESCRIPTION

The use of VC2 type single crystal material in the CP 215 compression mode dynamic pressure transducer makes this an extremely stable device.
The transducer is designed for monitoring or development testing of propulsion systems. It is fitted with an integral mineral insulated cable (triaxial) which is terminated with a coaxial Lemo connector from Vibro-Meter.

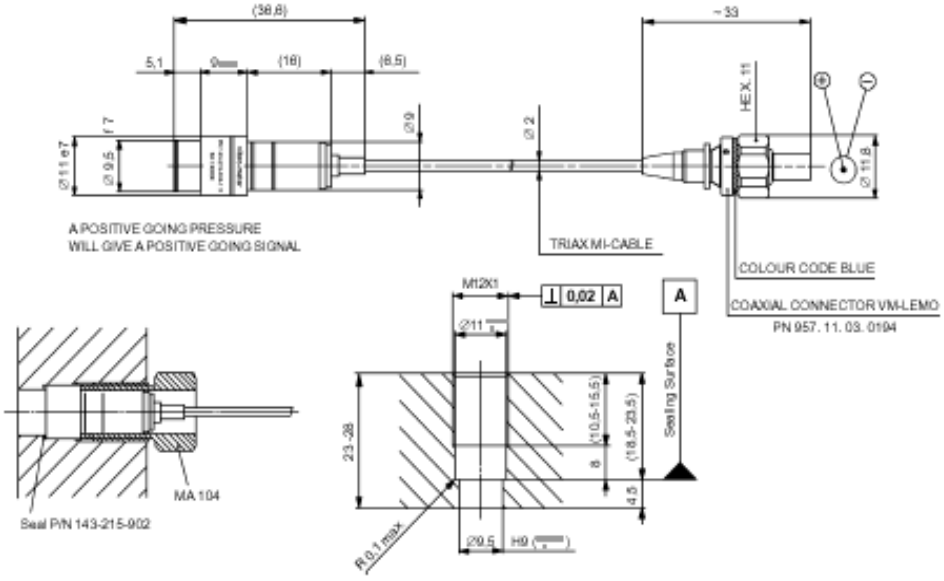

SPECIFICATIONS — CP 215

Input power requirements :
None

Signal transmission :
2 pole system insulated from casing, coaxial asymetrical connector, charge output

Signal processing :
Charge converter

OPERATING (at 23°C ± 5°C)

Sensitivity (at 2 Hz) :
25 pC/bar nominal

Dynamic measuring range (random) :
0.0005 bar to 250 bar

Overload capacity (spikes):
Up to 350 bar

Linearity :
±1% over dynamic measuring range

Acceleration sensitivity :
≤0.05 pC/g (≤0.002 bar/g)

Resonant frequency :
>80 kHz

Frequency response :
2 to 15,000 Hz ±5% (lower cutoff frequency is determined by the electronics used)

Internal insulation resistance :
Min. $10^{8}\Omega$ ($10^{6}\Omega$ at 750°C)

Capacitance :
- Transducer : 17.5 pF nominal pole/ground
- Integral cable : 310 pF nominal pole/ground

ENVIRONMENTAL

Temperature range :
-196°C to +750°C

Shock acceleration :
<2000 g peak (half sine,1 ms) along sensitive axis

Acoustic sensitivity on cable side (under 180 dB SPL) :
<0.005 bar

Corrosion, humidity :
Nimonic 90, AISI 304 L cable; case hermetically welded

Mounting :
- Flange : Diameter 11/9.5 mm x 9 mm

CALIBRATION :
Dynamic calibration at factory linearity 20, 40, 60, 80, 100 bar (60 Hz). No subsequent calibration necessary.

Typical Responses

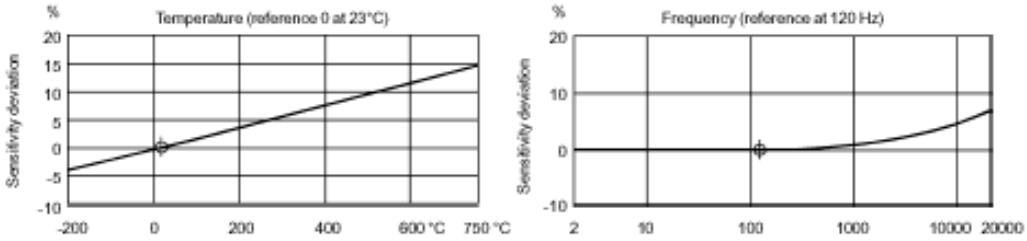

Accessories :

- Mounting adaptor : For mounting see drawing PZ-5084 (M12 X 1)
- Charge converter : See data sheet 278-002 TCC 1XX

Ordering Information :

- Description / Ordering No : CP 215 / 143-215-000-1X VM Lemo connector (coaxial)
  - 1 cable length 1.5 m
  - MA 104 / 809-104-000-0 Mounting Adaptor M12 X 1
  - Seal / 143-215-902-01 diameter 9.5/11 x 0.6

⚠ Due to the continual development of products, Vibro-Meter reserves the right to modify these specifications without forewarning.

vibro-meter

Head Office

Vibro-Meter SA, Rte de Moncor 4,
P.O. Box 1071, CH-1701 Fribourg, Switzerland
Phone : +41 26-407 11 11
Fax Industrial & Marine : +41 26-407 13 01
Fax Aerospace : +41 26-402 36 62
E-mail : vmsa@vibro-meter.ch
Internet : www.vibro-meter.com
www.meggitt.com

Sales Offices in :

- Germany
- France
- USA
- Canada
- Singapore
- United Kingdom
- Russia
- Ukraine

Agents in over 30 countries

Vibro-Meter is a member of the Meggitt Aerospace Systems Division

7. References

1. Munk, M. M.; and Powell, R. W.: Aeroassist Technology Planning for Exploration. *Advances in Aeronautical Sciences*, Vol. 105, Pt. 2, 2000, pp. 1073–1084. (Available as AAS 00-169.)

2. Lee, W.; D'Amario, L.; Roncoli, R.; and Smith, J.: Mission Design Overview for the Mars 2003/2005 Sample Return Mission. *Advances in Aeronautical Sciences*, Vol. 103, Pt. 1, 1999, pp. 85–102. (Available as AAS 99-305.)

3. Hoffman, S. J.; and Kaplan, D. I.; eds.: *Human Exploration of Mars: The Reference Mission of the NASA Mars Exploration Study Team*. NASA SP-6107, 1997.

4. Braun, R.; Powell, R.; Spencer, D.; and Mase, R.: *The Mars Surveyor 2001 Lander: A First Step Towards Precision Landing*. IAF 98-Q.3.03, 1998.

5. Lyons, D. T.: Aerobraking Magellan—Plan Versus Reality. *Advances in Astronautical Sciences*, Vol. 87, Pt. 2, 1994, pp. 663–680. (Available as AAS 94-118.)

6. Lyons, D. T.; Beerer, J. G.; Esposito, P.; Johnston, M. D.; and Willcockson, W. H.: Mars Global Surveyor: Aerobraking Mission Overview. *J. Spacecr. & Rockets*, vol. 36, no. 3, 1999, pp. 307–313.

7. Shane, R.; Rault, D. F. G.; and Tolson, R. H.: Mars Global Surveyor Aerodynamics for Maneuvers in Martian Atmosphere. AIAA-97-2509, June 1997.

8. Rault, D. F. G.; Cestero, F. J.; and Shane, R. W.: Spacecraft Aerodynamics During Aerobraking Maneuvers in Planetary Atmospheres. AIAA-96-1890, June 1996.

9. Wilmoth, R. G.; Rault, D. F. G.; Cheatwood, F. M.; Engelund, W. C.; and Shane, R. W.: Rarefied Aerothermodynamic Predictions for Mars Global Surveyor. *J. Spacecr. & Rockets*, vol. 36, no. 3, 1999, pp. 314–322.

10. Blanchard, R. C.; and Walberg, G. D.: *Determination of the Hypersonic-Continuum/Rarefied-Flow Drag Coefficient of the Viking Lander Capsule 1 Aeroshell From Flight Data.* NASA TP-1793, 1980.

11. Cancro, G. J.; Tolson, R. H.; and Keating, G. M.: *Operational Data Reduction Procedure for Determining Density and Vertical Structure of the Upper Atmosphere From Mars Global Surveyor Accelerometer Measurements*. NASA/CR-1998-208721, 1998.

12. Cestero, F. J.; and Tolson, R. H.: *Magellan Aerodynamic Characteristics During the Termination Experiment Including Thruster Plume-Free Stream Interactions.* NASA/CR-1998-206940, 1998.

13. King-Hele, D.: *Satellite Orbits in an Atmosphere: Theory and Applications.* Blackie & Sons, 1987, chap. 4.

14. Keating, G. M.; Bougher, S. W.; Zurek, R. W.; Tolson, R. H.; Cancro, G. J.; Noll, S. N.; Parker, J. S.; Schellenberg, T. J.; Shane, R. W.; Wilkerson, B. L.; Murphy, J. R.; Hollingsworth, J. L.; Haberle, R. M.; Joshi, M.; Pearl, J. C.; Conrath, B. J.; Smith, M. D.; Clancy, R. T.; Blanchard, R. C.; Wilmoth, R. G.; Rault, D. F.; Martin, T. Z.; Lyons, D. T.; Esposito, P. B.; Johnston, M. D.; Whetzel, C. W.; Justus, C. G.; and Babicke, J. M.: The Structure of the Upper Atmosphere of Mars: In Situ Accelerometer Measurements From Mars Global Surveyor. *Science*, vol. 279, no. 5357, 1998, pp. 1672–1676.

15. Milos, F. S.; Chen, Y.-K.; Congdon, W.; and Thornton, J. M.: Mars Pathfinder Entry Temperature Data, Aerothermal Heating, and Heatshield Material Response. *J. Spacecr. & Rockets*, vol. 36, no. 3, 1999, pp. 380–391.

16. Willcockson, W. H.: Mars Pathfinder Heatshield Design and Flight Experience. *J. Spacecr. & Rockets*, vol. 36, no. 3, 1999, pp. 374–379.

17. Moss, J. N.; Blanchard, R. C.; Wilmoth, R. G.; and Braun, R. D.: Mars Pathfinder Rarefied Aerodynamics: Computations and Measurements. *J. Spacecr. & Rockets*, vol. 36, no. 3, 1999, pp. 330–339.

18. Bhatnagar, M.; and Baliga, B. J.: Comparison of 6H-SiC, 3C-SiC, and Si for Power Devices. *IEEE Trans. Electron Devices*, vol. 40, no. 3, 1993, pp. 645–655.

19. Neudeck, P. G.; Larkin, D. J.; Starr, J. E.; Powell, J. A.; Salupo, C. S.; and Matus, L. G.: Greatly Improved 3C-SiC p-n Junction Diodes Grown by Chemical Vapor Deposition. *IEEE Electron Device Lett.*, vol. 14, no. 3, 1993, pp. 136–139.

20. Tairov, Y. M.; and Tsvetkov, V. F.: Investigation of Growth Processes of Ingots of Silicon Carbide Single Crystals. *J. Crys. Growth*, vol. 43, 1978, pp. 209–212.

21. Davis, R. F.; Carter, C. H., Jr.; and Hunter, C. E.: *Sublimation of Silicon Carbide To Produce Large, Device Quality Single Crystals of Silicon Carbide.* U.S. Patent 4,866,005, Sept. 12, 1989.

22. Barrett, D. L.; Seidensticker, R. G.; Gaida, W.; Hopkins, R. H.; and Choyke, W. J.: SiC Boule Growth by Sublimation Vapor Transport. *J. Crys. Growth*, vol. 109, no. 1–4, 1991, pp. 17–23.

23. Brandt, C. D.; Agarwal, A. K.; Augustine, G.; Burk, A. A.; Clarke, R. C.; Glass, R. C.; Hobgood, H. M.; McHugh, J. P.; McMullin, P. G.; Siegiej, R. R.; Smith, T. J.; Sriram, S.; Driver, M. C.; and Hopkins, R. H.: Advances in Silicon Carbide Device Processing and Substrate Fabrication for High Power Microwave and High Temperature Electronics. *Proceedings of the 21st International Symposium on Compound Semiconductors*, H. Goronkin and U. Mishra, eds., IOP Publ., 1994.

24. Powell, J. A.; Petit, J. B.; and Matus, L. G.: Advances in Silicon Carbide Chemical Vapor Deposition (CVD) for Semiconductor Device Fabrication. *Proceedings of the 1st International High Temperature Electronics Conference*, 1991.

25. Larkin, D. J.; Neudeck, P. G.; Powell, J. A.; and Matus, L. G.: Site-Competition Epitaxy for Superior Silicon Carbide Electronics. *Appl. Phys. Lett.*, vol. 65, no. 13, 1994, pp. 1659–1661.

26. Larkin, D. J.; Neudeck, P. G.; Powell, J. A.; and Matus, L. G.: Site-Competition Epitaxy for Controlled Doping of CVD Silicon Carbide. *Proceedings of the 5th International IOP Conference, No. 137: Silicon Carbide and Related Materials*, M. G. Spencer, R. P. Devaty, J. A. Edmond, M. A. Khan, R. Kaplan, and M. Rahman, eds., IOP Publ., 1994, pp. 51–54.

27. 4H-SiC-Wafer. http://www.sicrystal.de/4h.htm Assessed February 5, 2002.

28. 6H-SiC-Wafer. http://www.sicrystal.de/6h.htm Assessed February 5, 2002.

29. Lely-Platelets. http://www.sicrystal.de/lely.htm Assessed February 5, 2002.

30. Wax, Steven: Thin Film Coatings. http://www.darpa.mil/dso/trans/tmd.htm Assessed February 5, 2002.

31. Schaffer, Chris: Thermal Management Diamond. http://www.darpa.mil/dso/trans/tmd._2.htm Assessed February 5, 2002.

32. Butler, James E.: Thermal Management Diamond—Vapor Processing and Diamond Materials: Characterization, Diagnostics, and Modeling: Naval Research Laboratory. http://www.darpa.mil/dso/trans/tmd._4.htm. Assessed February 5, 2002.

33. Okojie, Robert S.; Lukco, Dorothy; Chen, Yuan L.; Spry, David; and Salupo, Carl: Reaction Kinetics of Thermally Stable Contact Metallization on 6H-SiC. *Symposium H: Silicon Carbide—Materials, Processing and Devices*, A. K. Agarwal, J. A. Cooper, Jr., E. Janzen, and M. Skowronski, eds., MRS Proceedings Volume 640, 2000, Paper 47.5.

34. Wilson, J. W.; Miller J.; Konradi, A.; and Cucinotta, F. A., eds.: *Shielding Strategies for Human Space Exploration*. NASA CP-3360, 1997.

8. Bibliography

Aeroassist

Braun, R.; Powell, R.; Spencer D.; and Mase, R.: *The Mars Surveyor 2001 Lander: A First Step Towards Precision Landing*. IAF 98-Q.3.03, 1998.

Hoffman, S. J.; and Kaplan, D. I.; eds.: *Human Exploration of Mars: The Reference Mission of the NASA Mars Exploration Study Team*. NASA SP-6107, 1997.

Lee, W.; D'Amario, L.; Roncoli, R.; and Smith, J.: Mission Design Overview for the Mars 2003/2005 Sample Return Mission. *Advances in Aeronautical Sciences*, Vol. 103, Pt. 1, 1999, pp. 85–102. (Available as AAS 99-305.)

Munk, M. M.; and Powell, R. W.: Aeroassist Technology Planning for Exploration. *Advances in Aeronautical Sciences*, Vol. 105, Pt. 2, 2000, pp. 1073–1084. (Available as AAS 00-169.)

Aerobraking

Blanchard, R. C.; and Walberg, G. D.: *Determination of the Hypersonic-Continuum/Rarefied-Flow Drag Coefficient of the Viking Lander Capsule 1 Aeroshell From Flight Data*. NASA TP-1793, 1980.

Cancro, G. J.; Tolson, R. H.; and Keating, G. M.: *Operational Data Reduction Procedure for Determining Density and Vertical Structure of the Upper Atmosphere From Mars Global Surveyor Accelerometer Measurements*. NASA/CR-1998-208721, 1998.

Cestero, F. J.; and Tolson, R. H.: *Magellan Aerodynamic Characteristics During the Termination Experiment Including Thruster Plume-Free Stream Interactions*. NASA/CR-1998-206940, 1998.

Keating, G. M.; Bougher, S. W.; Zurek, R. W.; Tolson, R. H.; Cancro, G. J.; Noll, S. N.; Parker, J. S.; Schellenberg, T. J.; Shane, R. W.; Wilkerson, B. L.; Murphy, J. R.; Hollingsworth, J. L.; Haberle, R. M.; Joshi, M.; Pearl, J. C.; Conrath, B. J.; Smith, M. D.; Clancy, R. T.; Blanchard, R. C.; Wilmoth, R. G.; Rault, D. F.; Martin, T. Z.; Lyons, D. T.; Esposito, P. B.; Johnston, M. D.; Whetzel, C. W.; Justus, C. G.; and Babicke, J. M.: The Structure of the Upper Atmosphere of Mars: In Situ Accelerometer Measurements From Mars Global Surveyor. *Science*, vol. 279, no. 5357, 1998, pp. 1672–1676.

King-Hele, D.: *Satellite Orbits in an Atmosphere: Theory and Applications*. Blackie & Sons, 1987, chap. 4.

Lyons, D. T.: Aerobraking Magellan—Plan Versus Reality. *Advances in Astronautical Sciences*, Vol. 87, Pt. 2, 1994, pp. 663–680. (Available as AAS 94-118.)

Lyons, D. T.; Beerer, J. G.; Esposito, P.; Johnston, M. D.; and Willcockson, W. H.: Mars Global Surveyor: Aerobraking Mission Overview. *J. Spacecr. & Rockets*, vol. 36, no. 3, 1999, pp. 307–313.

Milos, F. S.; Chen, Y.-K.; Congdon, W.; and Thornton, J. M.: Mars Pathfinder Entry Temperature Data, Aerothermal Heating, and Heatshield Material Response. *J. Spacecr. & Rockets*, vol. 36, no. 3, 1999, pp. 380–391.

Moss, J. N.; Blanchard, R. C.; Wilmoth, R. G.; and Braun, R. D.: Mars Pathfinder Rarefied Aerodynamics: Computations and Measurements. *J. Spacecr. & Rockets*, vol. 36, no. 3, 1999, pp. 330–339.

Rault, D. F. G.; Cestero, F. J.; and Shane, R. W.: Spacecraft Aerodynamics During Aerobraking Maneuvers in Planetary Atmospheres. AIAA-96-1890, June 1996.

Shane, R.; Rault, D. F. G.; and Tolson, R. H.: Mars Global Surveyor Aerodynamics for Maneuvers in Martian Atmosphere. AIAA-97-2509, June 1997.

Willcockson, W. H.: Mars Pathfinder Heatshield Design and Flight Experience. *J. Spacecr. & Rockets*, vol. 36, no. 3, 1999, pp. 374–379.

Wilmoth, R. G.; Rault, D. F. G.; Cheatwood, F. M.; Engelund, W. C.; and Shane, R. W.: Rarefied Aerothermodynamic Predictions for Mars Global Surveyor. *J. Spacecr. & Rockets*, vol. 36, no. 3, 1999, pp. 314–322.

SiC Technology and Diamond Thin Films

Baliga, B. J.: Power Semiconductor Devices for Variable-Frequency Drives. *Proceedings of IEEE*, vol. 82, no. 8, 1994, pp. 1112–1122.

Barrett, D. L.; Seidensticker, R. G.; Gaida, W.; Hopkins, R. H.; and Choyke, W. J.: SiC Boule Growth by Sublimation Vapor Transport. *J. Crys. Growth*, vol. 109, no. 1–4, 1991, pp. 17–23.

Bhatnagar, M.; and Baliga, B. J.: Comparison of 6H-SiC, 3C-SiC, and Si for Power Devices. *IEEE Trans. Electron Devices*, vol. 40, no. 3, 1993, pp. 645–655.

Brandt, C. D.; Agarwal, A. K.; Augustine, G.; Burk, A. A.; Clarke, R. C.; Glass, R. C.; Hobgood, H. M.; McHugh, J. P.; McMullin, P. G.; Siegiej, R. R.; Smith, T. J.; Sriram, S.; Driver, M. C.; and Hopkins, R. H.: Advances in Silicon Carbide Device Processing and Substrate Fabrication for High Power Microwave and High Temperature Electronics. *Proceedings of the 21st International Symposium on Compound Semiconductors*, H. Goronkin and U. Mishra, eds., IOP Publ., 1994.

Brown, D. M.; Ghezzo, M.; Kretchmer, J.; Downey, E.; Edmond, J.; Palmour, J.; Carter, C. H., Jr.; Gati, G.; Dasgupta, S.; Pimbley, J.; and Chow, P.: SiC Electronics for High Temperature Control Systems. *Proceedings of Government Microcircuit Applications Conference*, 1991.

Brown, D. M.; Ghezzo, M.; Kretchmer, J.; Downey, E.; Pimbley, J.; and Palmour, J.: SiC MOS Interface Characteristics. *IEEE Trans. on Electron Devices*, vol. 41, no. 4, 1994, pp. 618–620.

Brown, D. M.; Ghezzo, M.; Kretchmer, J.; Krishnamurthy, V.; Michon, G.; and Gati, G.: High Temperature Silicon Carbide Planar IC Technology and First Monolithic SiC Operational Amplifier IC. *Transactions of 2nd International High Temperature Electronics Conference*, 1994.

Cooper, J. A., Jr.; and Melloch, M. R.: NMOS Digital Integrated Circuits in 6H Silicon Carbide. WOCSEMMAD Conf., 1994.

Crofton, J.; Williams, J. R.; Bozack, M. J.; and Barnes, P. A.: A TiW High Temperature Ohmic Contact to n-Type 6H-SiC. *Proceedings of the 5th International IOP Conference, No. 137: Silicon Carbide and Related Materials*, M. G. Spencer, R. P. Devaty, J. A. Edmond, M. A. Khan, R. Kaplan, and M. Rahman, eds., IOP Publ., 1994, pp. 719–722.

Davis, R. F.; Carter, C. H., Jr.; and Hunter, C. E.: *Sublimation of Silicon Carbide To Produce Large, Device Quality Single Crystals of Silicon Carbide*. U.S. Patent 4,866,005, Sept. 12, 1989.

Davis, R. F.; Kelner, G.; Shur, M.; Palmour, J. W.; and Edmond, J. A.: Thin Film Deposition and Microelectronic and Optoelectronic Device Fabrication and Characterization in Monocrystalline Alpha and Beta Silicon Carbide. *Proc. IEEE*, vol. 79, no. 5, 1991, pp. 677–701.

Edmond, J. A.; Waltz, D. G.; Brueckner, S.; Kong, H.-S.; Palmour, J. W.; and Carter, C. H., Jr.: High Temperature Rectifiers in 6H-Silicon Carbide. *Proceedings of the 1st International High Temperature Electronics Conference*, 1991, pp. 207–212.

Fazi, C.; Dudley, M.; Wang, S.; and Ghezzo, M.: Issues Associated With Large-Area SiC Diodes With Avalanche Breakdown. *Proceedings of the 5th International IOP Conference, No. 137: Silicon Carbide and Related Materials*, M. G. Spencer, R. P. Devaty, J. A. Edmond, M. A. Khan, R. Kaplan, and M. Rahman, eds., IOP Publ., 1994, pp. 487–490.

Hingorani, N. G.; and Stahlkopf, K. E.: High-Power Electronics. *Sci. American*, vol. 269, no. 5, 1993, pp. 78–85.

Kimoto, T.; Itoh, A.; Urushidani, T.; Jang, S.; and Matsunami, H.: Step-Controlled Epitaxial Growth of SiC and Application to High-Voltage Schottky Rectifiers. *Proceedings of the 21st International Symposium on Compound Semiconductors*, no. 141, H. Goronkin and U. Mishra, eds., IOP Publ., 1994.

King, D. B.; and Thome, F. V.: Sessions X & XI. *Proceedings of 2nd International High Temperature Electronics Conference*, 1994.

Kong, H. S.; Glass, J. T.; and Davis, R. F.: Chemical Vapor Deposition and Characterization of 6H-SiC Thin Films on Off-Axis 6H-SiC Substrates. *J. Appl. Phys.*, vol. 64, no. 5, 1988, pp. 2672–2679.

Kordina, O.; Bergman, J. P.; Henry, A.; Janzen, E.; Savage, S.; Andre, J.; Ramberg, L. P.; Lindefelt, U.; Hermansson, W.; and Bergman, K.: A 4.5 kV 6H Silicon Carbide Rectifier. *Appl. Phys. Lett.*, vol. 67, no. 11, 1995, pp. 1561–1563.

Kordina, O.; Hallin, C.; Glass, R. C.; and Henry, A.: A Novel Hot-Wall CVD Reactor for SiC Epitaxy. *Proceedings of the 5th International IOP Conference, No. 137: Silicon Carbide and Related Materials*, M. G. Spencer, R. P. Devaty, J. A. Edmond, M. A. Khan, R. Kaplan, and M. Rahman, eds., IOP Publ., 1994, pp. 41–44.

Krishnamurthy, V.; Brown, D. M.; Ghezzo, M.; Kretchmer, J.; Hennessy, W.; Downey, E.; and Michon, G.: Planar Depletion-Mode 6H-SiC MOSFETs. *Proceedings of the 5th International IOP Conference, No. 137: Silicon Carbide and Related Materials*, M. G. Spencer, R. P. Devaty, J. A. Edmond, M. A. Khan, R. Kaplan, and M. Rahman, eds., IOP Publ., 1994, pp. 483–486.

Larkin, D. J.; Neudeck, P. G.; Powell, J. A.; and Matus, L. G.: Site-Competition Epitaxy for Superior Silicon Carbide Electronics. *Appl. Phys. Lett.*, vol. 65, no. 13, 1994, pp. 1659–1661.

Larkin, D. J.; Neudeck, P. G.; Powell, J. A.; and Matus, L. G.: Site-Competition Epitaxy for Controlled Doping of CVD Silicon Carbide. *Proceedings of the 5th International IOP Conference, No. 137: Silicon Carbide and Related Materials.*, M. G. Spencer, R. P. Devaty, J. A. Edmond, M. A. Khan, R. Kaplan, and M. Rahman, eds., IOP Publ., 1994, pp. 51–54.

Lomakina, G. A.: Electrical Properties of Various Polytypes of Silicon Carbide. *Silicon Carbide-1973*, R. C. Marshall, J. W. Faust, Jr., and C. E. Ryan, eds., Univ. of South Carolina Press, 1973, pp. 520–526.

Matsunami, H.; Shibahara, K.; Kuroda, N.; Yoo, W.; and Nishino, S.: VPE Growth of SiC on Step-Controlled Substrates. *Amorphous and Crystalline Silicon Carbide*, *Springer Proceedings in Physics, Vol. 34*, G. L. Harris and C. Y.-W. Yang, eds., Springer Verlag, 1989, pp. 34–39.

Neudeck, P. G.; Larkin, D. J.; Powell, J. A.; Matus, L. G.; and Salupo, C. S.: 2000 V 6H SiC p-n Junction Diodes Grown by Chemical Vapor Deposition. *Appl. Phys. Lett.*, vol. 64, no. 11, 1994, pp. 1386–1388.

Neudeck, P. G.; Larkin, D. J.; Starr, J. E.; Powell, J. A.; Salupo, C. S.; and Matus, L. G.: Electrical Properties of Epitaxial 3C- and 6H-SiC p-n Junction Diodes Produced Side-by-Side on 6H-SiC Wafers. *IEEE Trans. on Electron Devices*, vol. 41, no. 5, 1994, pp. 826–835.

Neudeck, P. G.; Larkin, D. J.; Starr, J. E.; Powell, J. A.; Salupo, C. S.; and Matus, L. G.: Greatly Improved 3C-SiC p-n Junction Diodes Grown by Chemical Vapor Deposition. *IEEE Electron Device Lett.*, vol. 14, no. 3, 1993, pp. 136–139.

Neudeck, P. G.; Petit, J. B.; and Salupo, C. S.: Silicon Carbide Buried-Gate Junction Field Effect Transistors for High-Temperature Power Electronic Applications. *Proceedings of 2nd International High Temperature Electronic Conference*, 1994.

Neudeck P. G.; and Powell, J. A.: Performance Limiting Micropipe Defects in Silicon Carbide Wafers. *IEEE Electron Device Lett.*, vol. 15, no. 2, 1994, pp. 63–65.

Nieberding, W. C.; and Powell, J. A.: High Temperature Electronic Requirements in Aeropropulsion Systems. *IEEE Trans. Ind. Electron.*, vol. 29, 1982, pp. 103–106.

Okojie, Robert S.; Lukco, Dorothy; Chen, Yuan L.; Spry, David; and Salupo, Carl: Reaction Kinetics of Thermally Stable Contact Metallization on 6H-SiC. *Symposium H: Silicon Carbide—Materials, Processing and Devices*, A. K. Agarwal, J. A. Cooper, Jr., E. Janzen, and M. Skowronski, eds., MRS Proceedings Volume 640, 2000, Paper 47.5.

Palmour, J. W.; Tsvetkov, V. F.; Lipkin, L. A.; and Carter, C. H., Jr.: Silicon Carbide Substrates and Power Devices. *Proceedings of the 21st International Symposium on Compound Semiconductors*, H. Goronkin and U. Mishra, eds., 1994, pp. 377–382.

Powell, J. A.; Larkin, D. J.; and Abel, P. B.: Surface Morphology of Silicon Carbide Epitaxial Films. *J. Electron. Mater.*, vol. 24, no. 4, 1995, pp. 295–302.

Powell, J. A.; Larkin, D. J.; Neudeck, P. G.; Yang, J. W.; and Pirouz, P.: Investigation of Defects in Epitaxial 3C-SiC, 4H-SiC, and 6H-SiC Films Grown on 6H-SiC Substrates. *Proceedings of the 5th International IOP Conference, No. 137: Silicon Carbide and Related Materials*, M. G. Spencer, R. P. Devaty, J. A. Edmond, M. A. Khan, R. Kaplan, and M. Rahman, eds., IOP Publ., 1994, pp. 161–164.

Powell, J. A.; Petit, J. B.; and Matus, L. G.: Advances in Silicon Carbide Chemical Vapor Deposition (CVD) for Semiconductor Device Fabrication, *Proceedings of the 1st International High Temperature Electronics Conference*, 1991.

Powell, J. A.; Pirouz, P.; and Choyke, W. J.: Growth and Characterization of Silicon Carbide Polytypes for Electronic Applications. *Semiconductor Interfaces, Microstructures, and Devices: Properties and Applications*, Z. C. Feng, ed., IOP Publ., 1993, pp. 257–293.

Przybylko, S. J.: Developments in Silicon Carbide for Aircraft Propulsion System Applications. AIAA-93-2581, June 1993.

Schaffer, W. J.; Negley, G. H.; Irvine, K. G.; and Palmour, J. W.: Conductivity Anisotropy in Epitaxial 6H and 4H SiC. *Proceedings of MRS Symposium-Diamond, SiC, and Nitride Wide-Bandgap Semiconductors*, Vol. 339, C. H. Carter, Jr., G. Gildenblatt, and S. Nakamura, eds., MRS, 1994, pp. 595–600.

Shenoy, J. N.; Lipkin, L. A.; Chindalore, G. L.; Pan, J.; Cooper, J. A., Jr.; Palmour, J. W.; and Melloch, M. R.: Electrical Characterization of the Thermally Oxidized SiO2/SiC Interface. *Proceedings of the 21st International Symposium on Compound Semiconductors*, no. 141, H. Goronkin and U. Mishra, eds., IOP Publ., 1994, pp. 449–454.

Sheppard, S. T.; Melloch, M. R.; and Cooper, J. A., Jr.: Characteristics of Inversion Channel and Buried-Channel MOS Devices in 6H-SiC. *IEEE Trans. Electron Devices*, vol. 41, no. 7, 1994, pp. 1257–1264.

Spencer, M. G.; Devaty, R. P.; Edmond, J. A.; Khan, M. A.; Kaplan, R.; and Rahman, M.: Chapter 6: Devices. *Proceedings of the 5th International IOP Conference, No. 137: Silicon Carbide and Related Materials*, M. G. Spencer, R. P. Devaty, J. A. Edmond, M. A. Khan, R. Kaplan, and M. Rahman, eds., IOP Publ., 1994, pp. 465–690.

Sriram, S.; Clarke, R. C.; Burk, A. A., Jr.; Hobgood, H. M.; McMullin, P. G.; Orphanos, P. A.; Siergiej, R. R.; Smith, T. J.; Brandt, C. D.; Driver, M. C.; and Hopkins, R. H.: X-Band Operation of SiC MESFET's on High Resistivity Substrates. *Fifty-Second IEEE Device Research Conference*, June 1994.

Sriram, S.; Clarke, R. C.; Hanes, M. H.; McMullin, P. G.; Brandt, C. D.; Smith, T. J.; Burk, A. A., Jr.; Hobgood, H. M.; Barrett, D. L.; and Hopkins, R. H.: SiC Microwave Power MESFETs: *Proceedings of the 5th International IOP Conference, No. 137: Silicon Carbide and Related Materials,* M. G. Spencer, R. P. Devaty, J. A. Edmond, M. A. Khan, R. Kaplan, and M. Rahman, eds., IOP Publ., 1994, pp. 491–494.

Stein, R. A.: Formation of Macrodefects in SiC. *Physica B*, vol. 185, no. 1–4, 1993, pp. 211–216.

Sze, S. M.: *Physics of Semiconductor Devices*, Second ed. John Wiley & Sons, 1981.

Tairov, Y. M.; and Tsvetkov, V. F.: Investigation of Growth Processes of Ingots of Silicon Carbide Single Crystals. *J. Crys. Growth*, vol. 43, 1978, pp. 209–212.

Trew, R. J.; Yan, J.-B.; and Mock, P. M.: The Potential of Diamond and SiC Electronic Devices for Microwave and Millimeter-Wave Power Applications. *Proc. IEEE*, vol. 79, no. 5, 1991, pp. 598–620.

Von Munch, W.: Silicon Carbide. *Physik der Elemete der IV, Gruppe und der III-V Verbindungen*, K.-H. Hellwege, ed., Springer-Verlag, 1982, pp. 132–142.

Wang, S.; Dudley, M.; Carter, C., Jr.; Asbury, D.; and Fazi, C.: Characterization of Defect Structures in SiC Single Crystals Using Synchrotron X-Ray Topography. *Proceedings of the Materials Research Society Symposium, Vol. 307: Applications of Synchrotron Radiation Techniques to Materials Science*, D. L. Perry, ed., MRS, 1993, pp. 249–254.

Weitzel, C. E.; Palmour, J. W.; Moore, K.; Carter, C. H., Jr.; and Nordquist, K. J.: SiC Microwave Power MESFET's and JFET's. *Proceedings of the 21st International Symposium on Compound Semiconductors*, no. 141, H. Goronkin and U. Mishra, eds., IOP Publ., 1994.

Wilson, J. W.; Miller J.; Konradi, A.; and Cucinotta, F. A., eds.: *Shielding Strategies for Human Space Exploration*. NASA CP-3360, 1997.

Xie, W.; Johnson, G. M.; Yang, Y.; Cooper, J. A., Jr.; Palmour, J. W.; Lipkin, L. A.; Melloch, M. R.; and Carter, C. H., Jr.: Cell Design and Peripheral Logic for Nonvolatile Random Access Memories in 6H-SiC. *Proceedings of the 21st International Symposium on Compound Semiconductors*, no. 141, H. Goronkin and U. Mishra, eds., IOP Publ., 1994, pp. 395–398.

Xie, W.; Pan, J.; Cooper, J. A., Jr.; and Melloch, M. R.: Monolithic Digital Integrated Circuits in 6H-SiC. *Proceedings of the 21st International Symposium on Compound Semiconductors*, no. 141, H. Goronkin and U. Mishra, eds., IOP Publ., 1994, pp. 455–458.

Yang, J.: SiC: Problems in Crystal Growth and Polytypic Transformation. Ph.D. Thesis, Case Western Reserve Univ., 1993.

REPORT DOCUMENTATION PAGE

Form Approved
OMB No. 0704-0188

1. AGENCY USE ONLY *(Leave blank)*	2. REPORT DATE	3. REPORT TYPE AND DATES COVERED
	April 2002	Technical Memorandum

4. TITLE AND SUBTITLE
Aerothermal Instrumentation Loads To Implement Aeroassist Technology in Future Robotic and Human Missions to MARS and Other Locations Within the Solar System

5. FUNDING NUMBERS
WU 713-81-70-050

6. AUTHOR(S)
Devendra S. Parmar and Qamar A. Shams

7. PERFORMING ORGANIZATION NAME(S) AND ADDRESS(ES)
NASA Langley Research Center
Hampton, VA 23681-2199

8. PERFORMING ORGANIZATION REPORT NUMBER
L-18123

9. SPONSORING/MONITORING AGENCY NAME(S) AND ADDRESS(ES)
National Aeronautics and Space Administration
Washington, DC 20546-0001

10. SPONSORING/MONITORING AGENCY REPORT NUMBER
NASA/TM-2002-211459

11. SUPPLEMENTARY NOTES
Parmar: ICASE, Langley Research Center, Hampton, VA; Shams: Langley Research Center, Hampton, VA.

12a. DISTRIBUTION/AVAILABILITY STATEMENT
Unclassified–Unlimited
Subject Category 35 Distribution: Standard
Availability: NASA CASI (301) 621-0390

12b. DISTRIBUTION CODE

13. ABSTRACT ***(Maximum 200 words)***

The strategy of NASA to explore space objects in the vicinity of Earth and other planets of the solar system includes robotic and human missions. This strategy requires a road map for technology development that will support the robotic exploration and provide safety for the humans traveling to other celestial bodies. Aeroassist is one of the key elements of technology planning for the success of future robot and human exploration missions to other celestial bodies. Measurement of aerothermodynamic parameters such as temperature, pressure, and acceleration is of prime importance for aeroassist technology implementation and for the safety and affordability of the mission. Instrumentation and methods to measure such parameters have been reviewed in this report in view of past practices, current commercial availability of instrumentation technology, and the prospects of improvement and upgrade according to the requirements. Analysis of the usability of each identified instruments in terms of cost for efficient weight-volume ratio, power requirement, accuracy, sample rates, and other appropriate metrics such as harsh environment survivability has been reported.

14. SUBJECT TERMS
Robotic; Human missions; Celestial bodies; Aerothermodynamic parameters; Instrumentation; Analysis; Power requirement; Accuracy; Appropriate metrics; Environment

15. NUMBER OF PAGES
44

16. PRICE CODE

17. SECURITY CLASSIFICATION OF REPORT	18. SECURITY CLASSIFICATION OF THIS PAGE	19. SECURITY CLASSIFICATION OF ABSTRACT	20. LIMITATION OF ABSTRACT
Unclassified	Unclassified	Unclassified	UL